

Synthesis, Structure, and Fluxionality of Strained Hypercoordinate Silicon-Bridged [1]Ferrocenophanes

Sara C. Bourke,^[a] Frieder Jäkle,^[a, b] Emira Vejzovic,^[a] Kin-Chung Lam,^[c] Arnold L. Rheingold,^[c] Alan J. Lough,^[a] and Ian Manners^{*,[a]}

Abstract: The first hypercoordinate sila[1]ferrocenophanes [fcSiMe(2-C₆H₄-CH₂NMe₂)] (**5a**) and [fcSi(CH₂Cl)(2-C₆H₄CH₂NMe₂)] (**5b**) (fc = (η^5 -C₅H₄)Fe(η^5 -C₅H₄)) were synthesized by low-temperature (−78 °C) reactions of Li[2-C₆H₄CH₂NMe₂] with the appropriate chlorinated sila[1]ferrocenophanes ([fcSiMeCl] (**1a**) and [fcSi(CH₂Cl)Cl] (**1d**), respectively). Single-crystal X-ray diffraction studies revealed pseudo-trigonal bipyramidal structures for both **5a** and **5b**, with one of the shortest reported Si⋯N distances for an sp³-hybridized nitrogen atom interacting with a tetraorganosilane detected for **5a** (2.776(2) Å). Elongated Si–C_{ipso} bonds *trans* to the donating NMe₂ arms (1.919(2) and 1.909(2) Å for **5a** and **5b**, respectively) were observed relative to both the non-*trans* bonds (**5a**: 1.891(2); **5b**: 1.879(2) Å) and the Si–C_{ipso} bonds of

the non-hypercoordinate analogues ([fcSiMePh] (**1b**): 1.879(4), 1.880(4) Å; [fcSi(CH₂Cl)Ph] (**1e**): 1.881(2), 1.884(2)). Solution-state fluxionality of **5a** and **5b**, suggestive of reversible coordination of the NMe₂ group to silicon, was demonstrated by means of variable-temperature NMR studies. The ΔG^\ddagger of the fluxional processes for **5a** and **5b** in CD₂Cl₂ were estimated to be 35.0 and 37.6 kJ mol^{−1}, respectively (35.8 and 38.3 kJ mol^{−1} in [D₈]toluene). The quaternization of **5a** and **5b** by MeOTf, to give [fcSiMe(2-C₆H₄CH₂NMe₃)](OTf) (**7a**-OTf) and [fcSi(CH₂Cl)(2-C₆H₄CH₂NMe₃)](OTf) (**7b**-OTf), respectively, supported the

reversibility of NMe₂ coordination at the silicon center as the source of fluxionality for **5a** and **5b**. Surprisingly, low room-temperature stability was detected for **5b** due to its tendency to intramolecularly cyclize and form the spirocyclic [fcSi(cyclo-CH₂NMe₂CH₂C₆H₄)]Cl (**9**-Cl). This process was observed in both solution and the solid state, and isolation and X-ray characterization of **9**-Cl was achieved. The model compound, [Fc₂Si(2-C₆H₄CH₂NMe₂)₂] (**8**), synthesized through reaction of [Fc₂SiCl₂] with two equivalents of Li[2-C₆H₄CH₂NMe₂] at −78 °C, showed a lack of hypercoordination in both the solid state and in solution (down to −80 °C). This suggests that either the reduced steric hindrance around Si or the unique electronics of the strained sila[1]ferrocenophanes is necessary for hypercoordination to occur.

Keywords: ferrocenophanes • fluxionality • hypervalent compounds • ring-opening polymerization • ring-strain

Introduction

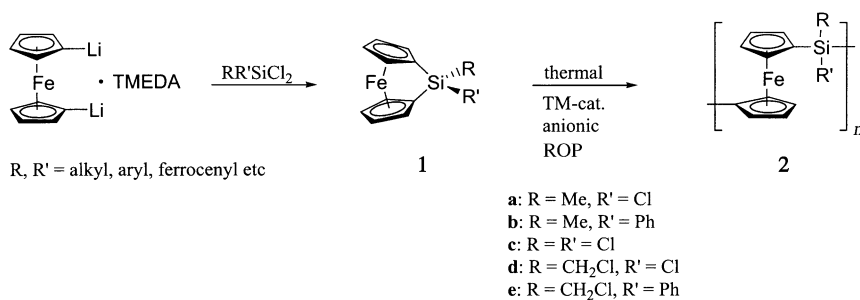
Hypercoordinate organosilicon compounds are of considerable interest in the field of silicon chemistry and have been studied extensively as models for the mechanism of nucleophilic substitution reactions at silicon and as possible intermediates in stereoisomerization processes.^[1] Pentacoordinate silicon species have been shown to display unusual characteristics that include enhanced reactivity in nucleophilic substitution reactions when compared with their tetracoordinate counterparts.^[2]

Strained silicon-bridged [1]ferrocenophanes **1**, synthesized by reaction of an appropriate dichlorosilane with dilithioferrocene [Eq. (1)], are an interesting class of tetracoordinate silanes. The presence of a strained ring distorts the geometry at the silicon center and results in a pseudo-tetrahedron with a contracted endocyclic C–Si–C angle and an expanded exocyclic C–Si–C angle.^[3]

[a] Prof. I. Manners, S. C. Bourke, Prof. Dr. F. Jäkle, E. Vejzovic, Dr. A. J. Lough
Department of Chemistry
University of Toronto
80 St. George Street, Toronto, ON M5S 3H6 (Canada)
Fax: (416) 978-6157
E-mail: imanners@chem.utoronto.ca

[b] Current address: Prof. Dr. F. Jäkle
Chemistry Department
Rutgers University
73 Warren Street, Newark, NJ 07102 (USA)
Fax: (973) 353-1264
E-mail: fjaekle@newark.rutgers.edu

[c] K.-C. Lam, Prof. A. L. Rheingold
Department of Chemistry and Biochemistry
University of Delaware
Newark, DE 19716 (USA)
Fax: (302) 831-6335
E-mail: arrrhein@udel.edu



The thermal,^[4] anionic^[5] and transition-metal-catalyzed^[6] ring opening polymerization (ROP) of these inherently strained species have led to high molecular weight polyferrocenylsilanes **2** that possess a range of interesting properties [Eq. (1)].^[7] In addition, the susceptibility of **1** towards ring-opening by electrophilic reagents and groups makes them useful in applications such as surface derivatization.^[8]

Previous investigation of the thermal ROP behavior of **1** has implicated cleavage of one of the monomer Si–C_{ipso} bonds as a key mechanistic step.^[9] In addition, our recent studies on the ROP of tin-bridged [1]ferrocenophanes **3** (see Scheme 1),^[10] have revealed that the introduction of neutral nucleophilic species such as amines leads to a dramatic enhancement of the rate of polymerization. The proposed initiation step for this process involves coordination of the nucleophile (Nu) to the bridging element (E) to give **4** and results in elongation of the E–C_{ipso} bond *trans* to the incoming nucleophile. Subsequent attack at the bridging atom of

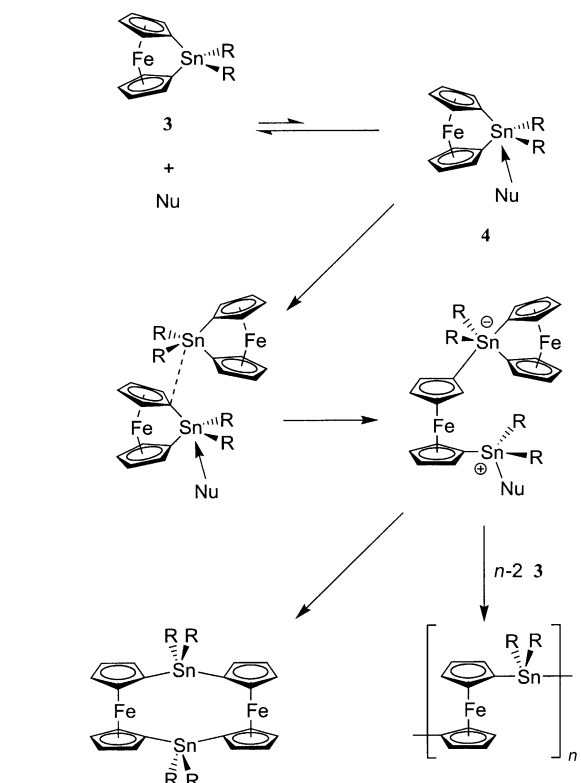
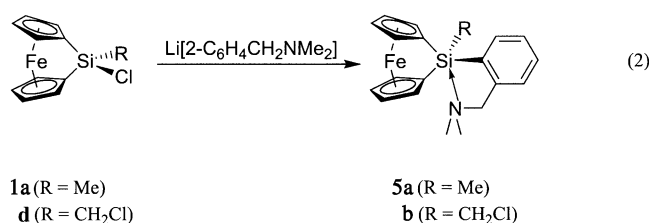
another ferrocenophane monomer results in chain propagation (Scheme 1).^[11] Based on these considerations we must further consider the possible mechanistic impact of amine nucleophiles on the thermal ROP of sila[1]ferrocenophanes **1**. It might be anticipated that trace amounts of such nucleophiles, present in monomers as a result of their synthesis from amine (tetramethylethylenediamine (TMEDA)) adducts of dilithioferrocene [Eq. (1)], could lead to ROP of **1** by a mechanism similar to that shown in Scheme 1 at elevated temperatures.

The synthesis and study of five-coordinate Group 14 bridged [1]ferrocenophanes would, in addition to being of intrinsic fundamental interest, be expected to provide further insight into these interesting mechanistic questions. In a previous communication we briefly reported the first hypercoordinate silicon-bridged [1]ferrocenophane, in which an intramolecularly donating amine group chelates to the Si center to give a pentacoordinate species.^[12] Herein we report full details of our work on the synthesis, structure and fluxionality of these species.

Results and Discussion

Synthesis and structure of the intramolecularly hypercoordinate sila[1]ferrocenophane [fcSiMe(2-C₆H₄CH₂NMe₂)] (**5a**):

Previously, chlorosilyl-bridged [1]ferrocenophanes have been shown to undergo nucleophilic substitution reactions in which alcohols and amines displace Cl in the presence of base, without cleavage of the Si–C_{ipso} bond.^[13] As noted previously,^[12] we have recently shown that, despite the fact that alkyl- and aryllithium reagents induce anionic ROP at room temperature, the low-temperature (–78 °C) reaction of a stoichiometric equivalent of an appropriate lithium reagent with chlorosilyl-bridged [1]ferrocenophanes can give selective substitution of Cl without evidence of polymerization. Thus, when [fcSiMeCl] (**1a**) (fc = (η⁵-C₅H₄)Fe(η⁵-C₅H₄)) was treated with Li[2-C₆H₄CH₂NMe₂] at –78 °C in THF the correspondingly substituted ferrocenophane [fcSiMe(2-C₆H₄CH₂NMe₂)] (**5a**) was formed as a red crystalline solid and isolated in 81 % yield after recrystallization from hexanes [Eq. (2)].



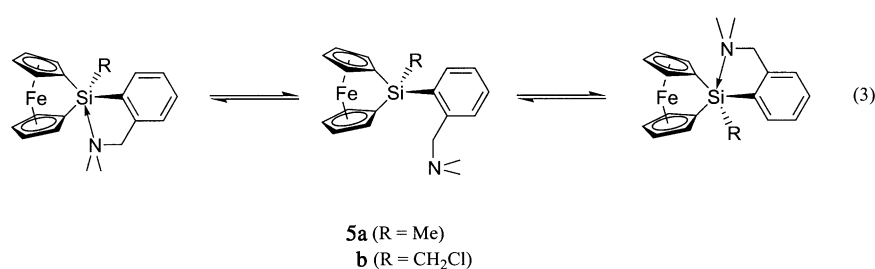
Scheme 1. Proposed mechanism for the nucleophilically-assisted ring-opening polymerization of stanna[1]ferrocenophanes (**3**).

The ¹H NMR spectrum of **5a** in C₆D₆ shows a resonance at δ = 8.29 ppm for the phenyl ring proton *ortho* to the Si center.

This is significantly downfield shifted compared with the analogous resonances for [fcSiMePh] (**1b**)^[14] ($\delta = 7.89$ ppm) and the non-hypercoordinate model compound 2-(SiMe₃)C₆H₄CH₂NMe₂ (**6**)^[15] ($\delta = 7.59$ ppm), and is typical for hypercoordinate silanes containing aryl substituents. The methylene resonance of the ligand appears at $\delta = 3.50$ ppm (cf. $\delta = 3.39$ ppm for **6**). The four resonances at $\delta = 4.45$, 4.38, 4.15, and 3.89 ppm are attributable to the cyclopentadienyl ring protons of **5a**, and indicate that hypercoordination in the solution state is dynamic rather than static; eight Cp resonances would be expected for a C₁-symmetric species in which the NMe₂ group does not dissociate from silicon. The presence of fluxionality is further supported by the fact that the methylene protons, as well as the two methyl groups present on the nitrogen center, are chemically and magnetically equivalent and appear as singlets in the room-temperature solution-state NMR spectrum of **5a**.

The ¹³C NMR spectrum of **5a** is also consistent with solution state fluxionality. However, the C_{ipso}-Cp resonance of **5a** is shifted significantly downfield relative to that of **1b** ($\delta = 37.4$ versus 32.1 ppm) and the ²⁹Si NMR signal of **5a** is shifted upfield relative to that of **1b** ($\delta = -13.9$ versus -7.7 ppm).^[14] These shifts are both indicative of electron donation at the silicon center and demonstrate that, despite fluxionality, there is a significant Si...N interaction in solution.

The nature of the fluxional behavior of **5a** was further investigated by variable-temperature NMR spectroscopy. Monitoring of the ²⁹Si NMR shift of **5a** in solution ([D₈]toluene) showed that the signal was shifted to increasingly high field as the temperature decreased ($\delta = -13.4$ (+80 °C), -13.8 (+25 °C), -15 ppm (-80 °C)). This further suggests the existence of an equilibrium between coordinated and uncoordinated species. Previous work on pentacoordinate silicon species containing the 2-C₆H₄CH₂NMe₂ ligand has shown that a fast exchange process [Eq. (3)] is likely, based on the upfield shift of the low-temperature resonance.^[15]



In contrast to the spectrum at 25 °C (vide supra), the ¹H NMR spectrum at -100 °C (in [D₈]toluene) shows two distinct resonances ($\delta = 4.39$ and 2.56 ppm) for the methylene protons of the intramolecularly coordinating ligand as well as for the methyl groups attached to the nitrogen center ($\delta = 2.10$ and 1.76 ppm). This is expected when the lifetimes of the enantiomeric C₁-symmetric pentacoordinate species are longer than the NMR time scale. The coalescence temperature of the dimethylamino methyl resonances was found to be -88 °C

on a 400 MHz spectrometer, and the free energy of the exchange process was estimated to be $\Delta G^\ddagger_{[\text{D}_8]\text{toluene}} = 35.8$ kJ mol⁻¹, based on the chemical shift difference of 136 Hz at -100 °C.^[16] Coalescence of the methylene resonances as well as three of the four Cp resonances could also be observed over the temperature range studied (-100 to 25 °C).^[17]

It was expected that the 'open' species in which the dimethylamino group is not coordinated to the silicon center would be more stabilized in a more polar solvent (e.g. CD₂Cl₂), and would facilitate the exchange process illustrated in Equation (3). Indeed, in CD₂Cl₂ the barrier to this exchange process was found to be slightly lower ($\Delta G^\ddagger_{\text{CD}_2\text{Cl}_2} = 35.0$ kJ mol⁻¹). Coalescence of the NMe₂ resonances ($\delta = 2.19$ and 1.87 ppm at -106 °C) was seen (400 MHz) at -92 °C and that of the methylene protons ($\delta = 4.00$ and 2.92 ppm at -106 °C) at -69 °C (Figure 1).

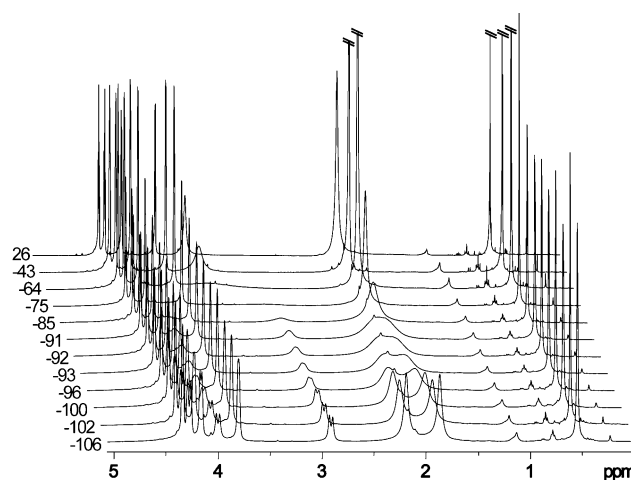


Figure 1. Variable-temperature ¹H NMR spectra of **5a** (CD₂Cl₂) at -106 , -102 , -100 , -96 , -93 , -92 , -91 , -85 , -75 , -64 , -43 , and 26 °C that show its fluxionality in solution.

Below -92 °C discrete resonances for all of the protons were observed, except for those due to free rotation of the methyl groups and for those associated with two of the eight Cp environments. As the coalescence temperature is dependent both on the field of the instrument and the ultimate chemical shift difference under static conditions, decoalescence of these Cp protons at low temperature was likely unobservable due to the similarity of their chemical shifts. The coupling between the two protons on the methylene bridge of the intramolecularly donating aryl substituent was found to be $^2J(\text{H,H}) = 12.6$ Hz.

A single-crystal X-ray diffraction study of **5a** confirmed the attachment of the chelating 2-C₆H₄CH₂NMe₂ ligand to the silicon center in the solid state without cleavage of the Si-C_{ipso} bond (Figure 2). Selected bond lengths and angles are given in Table 1. The pseudo-trigonal-bipyramidal structure shows one

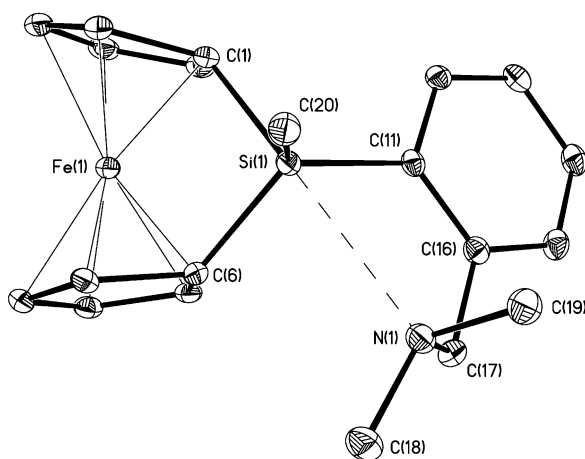


Figure 2. Molecular structure of **5a** showing thermal ellipsoids at 30% probability.

Table 1. Selected bond lengths [Å] and angles [°] for **5a**.

Si(1)–N(1)	2.7763(17)	Si(1)–C(6)	1.8909(19)
Si(1)–Fe(1)	2.7584(6)	Si(1)–C(11)	1.883(2)
Si(1)–C(1)	1.919(2)	Si(1)–C(20)	1.865(2)
C(1)–Si(1)–C(6)	93.68(8)	Si(1)–C(11)–C(16)	122.72(14)
C(1)–Si(1)–C(11)	103.76(9)	C(11)–C(16)–C(17)	118.91(18)
C(1)–Si(1)–C(20)	106.58(9)	N(1)–C(17)–C(16)	110.72(16)
C(6)–Si(1)–C(11)	113.36(9)	C(17)–N(1)–C(18)	111.19(16)
C(6)–Si(1)–C(20)	112.90(9)	C(17)–N(1)–C(19)	110.54(16)
C(11)–Si(1)–C(20)	121.74(9)	C(18)–N(1)–C(19)	110.52(16)
N(1)–Si(1)–C(1)	174.63(7)	Si(1)–N(1)–C(17)	91.54(11)
N(1)–Si(1)–C(6)	83.88(7)	Si(1)–N(1)–C(18)	117.60(13)
N(1)–Si(1)–C(11)	73.00(7)	Si(1)–N(1)–C(19)	113.96(12)
N(1)–Si(1)–C(20)	78.78(7)		

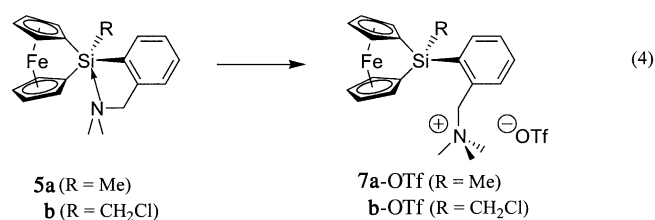
of the shortest reported Si⋯N distances for an sp³-hybridized nitrogen atom interacting with a tetraorganosilane (2.776(2) Å).^[18]

Its value is at the upper limit for donor–acceptor complexes and at the lower limit of Coulomb-dominated donor–acceptor bonding.^[19] The small endocyclic C(1)–Si(1)–C(6) angle and the large exocyclic C–Si–R angles may account for this relatively short distance. Another factor that could influence this interaction is the unusual electronic nature of strained ferrocenophanes.^[20] The Si–C_{ipso} bond *trans* to the donating nitrogen atom (1.919(2) Å) is elongated in comparison with the other Si–C_{ipso} bond (1.891(2) Å) and those found in the analogous four-coordinate species **1b** (1.879(4) and 1.880(4) Å).^[21] This was of particular interest as it seemed to indicate that an incoming nucleophile at the silicon bridge leads to weakening of this ‘*trans*’ Si–C_{ipso} bond. The overall geometry of the structure is intermediate between a trigonal bipyramid and a capped tetrahedron. If one compares the structure of **5a** to an ideal trigonal bipyramid one finds that the N(1)–Si(1)–C(1) angle of 174.63(7)° approaches the theoretical value of 180° expected for axial substituents. The C(11)–Si(1)–C(20) angle of 121.74(9)° between the methyl and aryl substituents is also close to the expected equatorial angle of 120° and is significantly larger than that found in other sila[1]ferrocenophanes (cf. 112.4(2)° for **1b**). Consequently, the endocyclic C(1)–Si–C(6) angle of 93.68(8)° is smaller than

that found in other silicon-bridged ferrocenophanes (cf. 96.2(2)° for **1b**) and approaches the ideal 90° angle. The sum of the equatorial angles around the silicon center, 347.96°, corresponds to a value of 61.8% of pentacoordination character TBP_e.^[22] The tilt angle α between the planes of the Cp rings (21.27(1)°) is slightly larger than that in other silicon-bridged [1]ferrocenophanes and is a logical result of the contraction of the C(1)–Si–C(6) angle. Also, the average β angle (between each Cp plane and the corresponding Si–C_{ipso} bond) of 35.9° is slightly smaller than that in other sila[1]ferrocenophanes. Finally, it has previously been postulated that an Fe⋯Si interaction plays a role in the electronic nature of sila[1]ferrocenophanes, with the Fe center donating electron density to the Si center.^[3a,b] In this case, a decrease in this interaction, manifested in a lengthening of the distance between these nuclei, could be expected due to the Si⋯N intramolecular donation. The Fe⋯Si distance of 2.758 Å for **5a** is indeed longer than that for the non-hypercoordinate analogue **1b** (2.692 Å).

Previous studies of the electronic nature of [1]ferrocenophanes by UV/Vis spectroscopy as well as by extended Hückel MO calculations have shown that the energy of the HOMO–LUMO transition is highly dependent upon the α angle between the cyclopentadienyl rings in the ferrocene moiety.^[23] Indeed, as the Cp rings tilt there is a decrease in the HOMO–LUMO gap that leads to a bathchromic shift of the corresponding electronic transition.^[3, 23] In addition, the decreased symmetry leads to an increase in the intensity of these Laporte forbidden d–d transitions. The maximum for the d–d transition in **5a** ($\lambda_{\max} = 482$ nm, $\epsilon = 276$) is slightly blue-shifted relative to that of **1b** ($\lambda_{\max} = 487$ nm, $\epsilon = 308$) despite a similar solid-state tilt angle ($\alpha = 21.0^\circ$ for **1b** versus 21.27° for **5a**). This deviation may be due to the influence of the novel Si⋯N interaction.

Quaternization of [fcSiMe(2-C₆H₄CH₂NMe₂)] (5a): Reaction of **5a** with MeOTf at 0°C in toluene leads to suppression of pentacoordination and the synthesis of the quaternized cation **7a** [Eq. (4)]. The quaternization of the nitrogen atom is



indicated by a pronounced downfield shift of its methyl and methylene proton resonances in the NMR spectrum ($\delta = 2.83$ and 4.91 versus 1.97 and 3.50 ppm for **5a**). In addition, the ¹³C C_{ipso} and ²⁹Si NMR shifts for **7a** ($\delta = 31.9$ and -9.2 ppm, respectively) are similar to those found for **1b** and are indicative of loss of the Si⋯N interaction.

A single crystal X-ray diffraction study of **7a-OTf** showed that quaternization of the nitrogen atom results in this moiety bending away from the silicon center (Figure 3, Table 2). In fact the Si(1)–C(11)–C(12) angle at the C_{ipso} of the phenyl ring

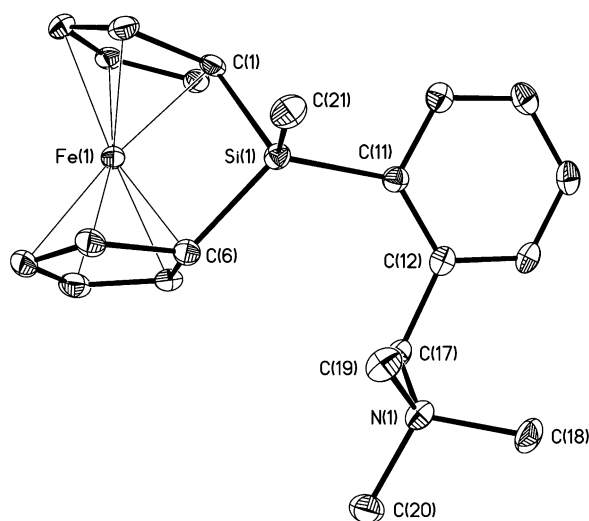


Figure 3. Molecular structure of **7a** showing thermal ellipsoids at 30% probability.

Table 2. Selected bond lengths [Å] and angles [°] for **7a**-OTf.

Si(1)–Fe(1)	2.6932(12)	Si(1)–C(11)	1.885(4)
Si(1)–C(1)	1.883(4)	Si(1)–C(21)	1.857(5)
Si(1)–C(6)	1.882(4)		
C(1)–Si(1)–C(6)	96.10(18)	N(1)–C(17)–C(12)	117.0(3)
C(1)–Si(1)–C(11)	112.01(17)	C(17)–N(1)–C(18)	111.5(3)
C(1)–Si(1)–C(21)	107.87(19)	C(17)–N(1)–C(19)	110.7(3)
C(6)–Si(1)–C(11)	116.34(19)	C(17)–N(1)–C(20)	107.6(3)
C(6)–Si(1)–C(21)	113.0(2)	C(18)–N(1)–C(19)	108.1(3)
C(11)–Si(1)–C(21)	110.5(2)	C(18)–N(1)–C(20)	109.4(3)
Si(1)–C(11)–C(12)	130.3(3)	C(19)–N(1)–C(20)	109.4(3)
C(11)–C(12)–C(17)	122.6(3)		

is wider than the expected trigonal angle (130.3(3) versus 120°), possibly to accommodate the steric bulk of the $\text{CH}_2\text{NMe}_3^+$ arm in the absence of a $\text{Si}\cdots\text{N}$ interaction. The environment around the cationic nitrogen center is essentially tetrahedral with an average C–N–C angle of 109.5°. The environment around the silicon center is much closer to a tetrahedral environment (average C–Si–C angle 109.3°) than in **5a**, with the major deviations being the endocyclic C(1)–Si–C(6) angle of 96.10(5)°, constrained as expected due to the presence of the ferrocenophane ring, and the correspondingly expanded exocyclic angles, as large as 116.34(19)° (C(11)–Si–C(21)). The tilt angle (α) of 20.6° between the planes of the Cp rings is typical for a silicon-bridged ferrocenophane.^[3]

Synthesis and characterization of $[\text{Fc}_2\text{Si}(2\text{-C}_6\text{H}_4\text{CH}_2\text{NMe}_2)_2]$ (**8**):

The strength of the $\text{Si}\cdots\text{N}$ interaction in **5a** led to speculation over the possible influence of the unusual structure of the strained sila[1]ferrocenophane upon the observed hypercoordination. The model compound investigated to probe this issue further was $[\text{Fc}_2\text{Si}(2\text{-C}_6\text{H}_4\text{CH}_2\text{NMe}_2)_2]$ (**8**). This species was prepared through the reaction of Fc_2SiCl_2 with two equivalents of $\text{Li}[2\text{-C}_6\text{H}_4\text{CH}_2\text{NMe}_2]$ in THF at -78°C . Initial attempts to substitute only one of the Si–Cl functionalities failed due to the preferential formation of the disubstituted product, as observed by ^1H NMR spectroscopy. A second equivalent was

added to complete conversion to $[\text{Fc}_2\text{Si}(2\text{-C}_6\text{H}_4\text{CH}_2\text{NMe}_2)_2]$ (**8**), which was then isolated in 27% yield.

The ^1H NMR spectrum of **8** in C_6D_6 showed the *ortho* proton resonance of the phenyl rings at $\delta = 7.96$ ppm, comparable to the shift found in tetracoordinate organosilanes that possess aryl substituents ($\delta = 7.89$ ppm for **1b**, $\delta = 7.59$ ppm for **6**), and was indicative of a lack of hypercoordination in solution.^[1a] The resonances for the cyclopentadienyl protons appeared at $\delta = 4.60$, 4.34, and 3.93 ppm and are typical for ferrocenyl substituents on silicon.

A variable-temperature (VT) NMR study in CD_2Cl_2 was undertaken to explore the possibility of solution-state hypercoordination at sub-ambient temperatures. Although broadening of the methylene resonance and one of the Cp resonances was found at -80°C , there was no observation of hypercoordination on the NMR timescale at this temperature.

The solid-state structure of **8** was investigated by means of a single-crystal X-ray diffraction study (Figure 4, Table 3). The

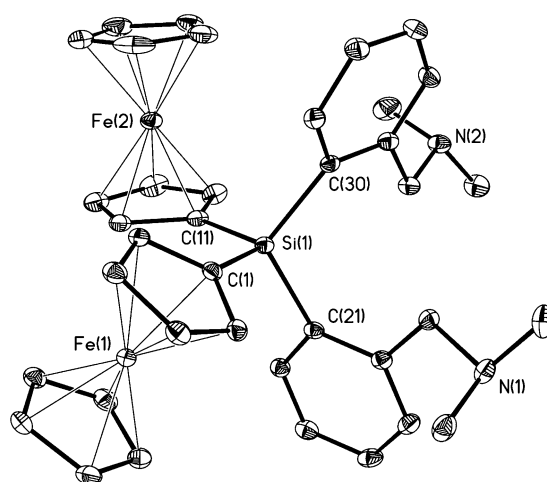


Figure 4. Molecular structure of **8** showing thermal ellipsoids at 30% probability.

Table 3. Selected bond lengths [Å] and angles [°] for **8**.

Si(1)–C(1)	1.862(2)	Si(1)–C(21)	1.891(2)
Si(1)–C(11)	1.8742(19)	Si(1)–C(30)	1.8952(19)
C(1)–Si(1)–C(11)	109.61(9)	C(11)–Si(1)–C(21)	109.28(9)
C(1)–Si(1)–C(21)	106.92(9)	C(11)–Si(1)–C(30)	110.35(8)
C(1)–Si(1)–C(30)	107.12(8)	C(21)–Si(1)–C(30)	113.44(8)

lack of hypercoordination in the structure further supported the variable temperature data. The environment at silicon is approximately tetrahedral with C–Si–C angles ranging from 106.92(9)° (C(1)–Si–C(21)) to 113.44(8)° (C(21)–Si–C(30)) and averaging 109.5°.

Attempted synthesis of $[\text{fcSiCl}(2\text{-C}_6\text{H}_4\text{CH}_2\text{NMe}_2)]$: The lack of hypercoordination found for **8** seemed to indicate that either the decreased steric crowding around silicon, or the unusual electronic structure associated with a strained ferro-

cenophane system, is necessary for hypercoordination to be favorable. Moreover, despite the considerable strength of the Si...N interaction found for **5a**, we anticipated that it should be possible to create an even stronger interaction in a strained sila[1]ferrocenophane system through introduction of an electron-withdrawing substituent at silicon. However, reaction of a stoichiometric equivalent of Li[2-C₆H₄CH₂NMe₂] with [fcSiCl₂] (**1c**) at -78 °C led to a complex reaction mixture. It is likely that the desired monosubstituted product [fcSiCl(2-C₆H₄CH₂NMe₂)] is, once generated, highly reactive towards further substitution. Such disubstitution is preceded by the synthesis of **8** where the disubstituted product is formed exclusively. In addition, we would expect [fcSiCl(2-C₆H₄CH₂NMe₂)] to be particularly reactive towards ring-opening due to an enhanced Si...N interaction and subsequent weakening of the *trans* Si-C_{ipso} bond in the presence of the electron-withdrawing Cl group.

Synthesis and characterization of [fcSi(CH₂Cl)(2-C₆H₄CH₂NMe₂)] (5b**):** The problems inherent in the selective reaction of one of the Si-Cl functionalities in [fcSiCl₂] led us to the synthesis of a sila[1]ferrocenophane that would provide the Si-Cl functionality necessary for substitution by Li[2-C₆H₄CH₂NMe₂], as well as a less reactive, electron-withdrawing group. The chloromethyl functionality was chosen as a result of previous work in our group that indicated that it was rather inert as a functional group on sila[1]ferrocenophanes.^[24] The new ferrocenophane [fcSi(CH₂Cl)Cl] (**1d**) was therefore synthesized through reaction of fLi₂· $\frac{2}{3}$ TMEDA with a slight excess of (CH₂Cl)SiCl₃ at -78 °C in Et₂O [Eq. (2)]. This sila[1]ferrocenophane was purified by recrystallization from hexanes and isolated in 68% yield. ¹H and ¹³C NMR spectra were consistent with an unsymmetrically substituted Si center.^[14] Four distinct Cp resonances were observed in the ¹³C NMR spectrum, and the ¹H NMR spectrum showed three multiplets for the Cp protons; one with double the intensity and attributable to two unresolved signals. Indeed, the ¹³C NMR spectrum for this compound shows two distinct but extremely similar Cp carbon environments with resonances at δ = 79.1 and 79.0 ppm. The ²⁹Si NMR spectrum showed one Si environment with a shift of δ = -0.3 ppm.

Subsequent reaction of **1d** with 1.1 equivalents of Li[2-C₆H₄CH₂NMe₂] at -78 °C in THF, followed by quenching of any excess lithium salt with Me₃SiCl at -30 °C, yielded the desired product **5b** in 66% yield. This species was characterized by ¹H, ¹³C, and ²⁹Si NMR spectroscopy, mass spectrometry, and elemental analysis. To provide comparative structural information, the non-hypercoordinate analogue of **5b**, [fcSi(CH₂Cl)Ph] (**1e**), was prepared by the reaction of PhLi with **1d** and was similarly characterized. In a manner similar to the case of **5a**, the ¹H and ¹³C NMR spectra of **5b** were consistent with fluxionality in solution, and showed four Cp resonances as well as degenerate methylene proton and NMe₂ methyl resonances. However, the methylene proton resonance is rather broad, even at room temperature, as might be expected in the presence of the more electrophilic silicon and an increased Si...N interaction. Also indicative of increased interaction between these two nuclei is the upfield

shifted ²⁹Si NMR resonance at δ = -14.8 ppm (cf. δ = -13.9 ppm for **5a**, δ = -10.4 ppm for **1e**). A higher ΔG^\ddagger value for the exchange process as well as a shorter Si...N distance might also be anticipated.

Investigations of **5b** by VT-NMR spectroscopy did indeed show the anticipated increase in the value of $\Delta G^\ddagger_{\text{CD}_2\text{Cl}_2}$. The solution was raised from -96 °C^[17] to room temperature and ¹H NMR spectra (300 MHz) were acquired at a variety of temperatures (Figure 5). As for **5a** in CD₂Cl₂, we observe a

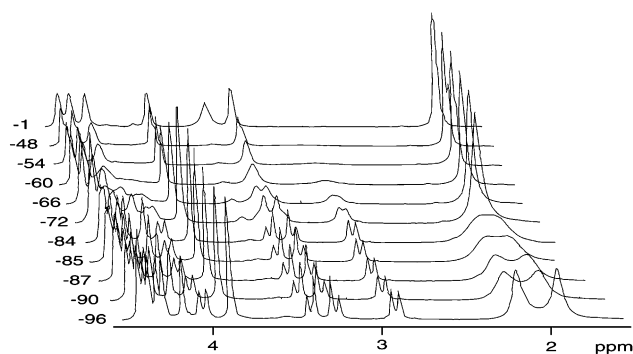


Figure 5. Variable-temperature ¹H NMR spectra of **5b** (CD₂Cl₂) at -96, -90, -87, -85, -84, -72, -66, -60, -54, -48, and -1 °C showing its fluxionality in solution.

coalescence temperature for the two methylene protons (-45 °C) and clear doublets below -72 °C (δ = 4.05 and 2.90 ppm at -96 °C, ²J(H,H) = 12.9 Hz). In addition, we see coalescence for three of the four pairs of Cp protons (-60, -72, and -78 °C), the protons of the CH₂Cl group (-60 °C) and the protons of the methyl groups on the intramolecularly coordinating NMe₂ group (-84 °C). In the case of the CH₂Cl protons some second-order effects are seen due to the proximity of the shifts of the interacting protons (δ = 3.40 and 3.26 ppm at -96 °C, ²J(H,H) = 13.2 Hz). The most clearly discernable coalescence temperature is that seen for the methyl groups on the NMe₂ group (δ = 2.18 and 1.94 ppm at -96 °C). Numerous spectra were acquired at the lower end of the temperature range and the flattening of the merged peaks characteristic of coalescence can clearly be seen for these protons at -84 °C. The free energy of the exchange process was calculated from this coalescence temperature, in combination with the separation of the methyl resonances at -96 °C (73.5 Hz), to be $\Delta G^\ddagger_{\text{CD}_2\text{Cl}_2}$ = 37.6 kJ mol⁻¹; slightly higher than that for **5a** in the same solvent. The magnitude of this value is indicative of a stronger Si...N interaction in solution for **5b** than for **5a**.

The solid-state structure of **5b** was investigated by single crystal X-ray diffraction (Figure 6, Table 4) and compared with that of **5a** as well as that of its non-hypercoordinate analogue (**1e**) (Figure 7, Table 5). The structure of **5b** does show a Si...N interaction in the solid state, with a distance of 2.876 Å, slightly longer than that seen for **5a**, despite the stronger interaction demonstrated by VT-NMR spectroscopy. The space group for the structure is C2/c rather than P2₁/n (for **5a**) and packing effects could be responsible for the observed lengthening. As seen with **5a** there is a lengthening of the Si-C_{ipso} bond *trans* to the incoming NMe₂ group (1.909(2)

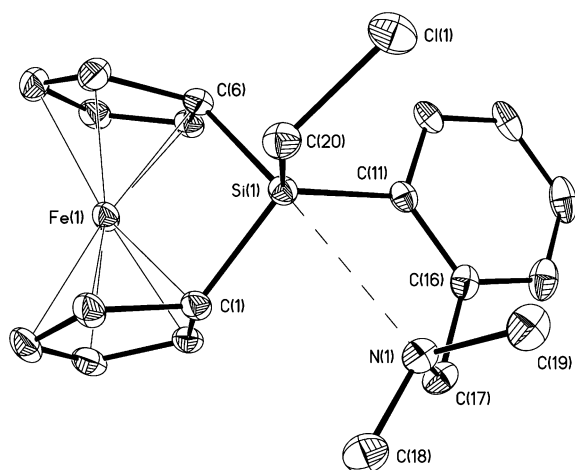


Figure 6. Molecular structure of **5b** that shows thermal ellipsoids at 30% probability.

Table 4. Selected bond lengths [\AA] and angles [$^\circ$] for **5b**.

Si(1)–N(1)	2.876(2)	Si(1)–C(6)	1.909(2)
Si(1)–Fe(1)	2.7402(7)	Si(1)–C(11)	1.870(2)
Si(1)–C(1)	1.879(2)	Si(1)–C(20)	1.884(2)
C(1)–Si(1)–C(6)	94.39(10)	Si(1)–C(11)–C(16)	122.53(17)
C(1)–Si(1)–C(11)	115.06(10)	C(11)–C(16)–C(17)	119.3(2)
C(1)–Si(1)–C(20)	110.46(10)	N(1)–C(17)–C(16)	110.03(19)
C(6)–Si(1)–C(11)	106.41(10)	C(17)–N(1)–C(18)	110.71(19)
C(6)–Si(1)–C(20)	107.19(11)	C(17)–N(1)–C(19)	109.7(2)
C(11)–Si(1)–C(20)	119.77(10)	C(18)–N(1)–C(19)	110.5(2)
N(1)–Si(1)–C(1)	81.10(8)	Si(1)–N(1)–C(17)	87.19(13)
N(1)–Si(1)–C(6)	173.54(9)	Si(1)–N(1)–C(18)	116.25(15)
N(1)–Si(1)–C(11)	71.72(8)	Si(1)–N(1)–C(19)	119.84(16)
N(1)–Si(1)–C(20)	78.84(9)		

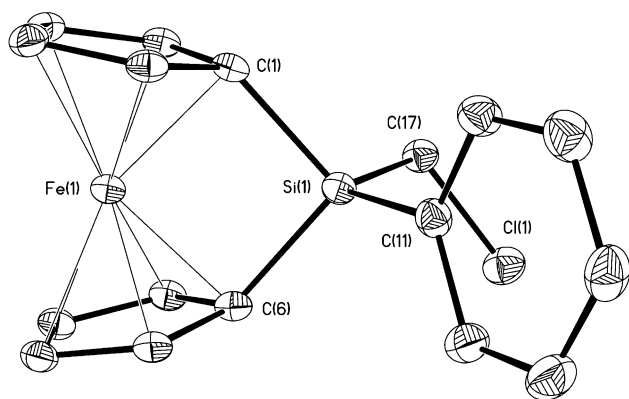


Figure 7. Molecular structure of **1e** that shows thermal ellipsoids at 30% probability.

Table 5. Selected bond lengths [\AA] and angles [$^\circ$] for **1e**.

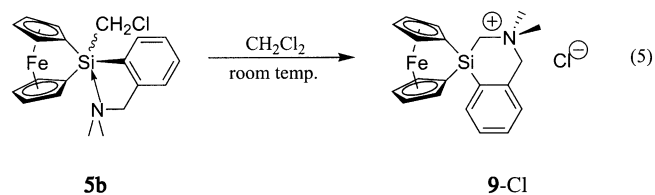
Si(1)–Fe(1)	2.6903(7)	Si(1)–C(11)	1.857(2)
Si(1)–C(1)	1.881(2)	Si(1)–C(17)	1.875(2)
Si(1)–C(6)	1.884(2)		
C(1)–Si(1)–C(6)	97.04(10)	C(6)–Si(1)–C(11)	110.92(11)
C(1)–Si(1)–C(11)	111.72(11)	C(6)–Si(1)–C(17)	113.37(11)
C(1)–Si(1)–C(17)	108.49(11)	C(11)–Si(1)–C(17)	114.05(11)

versus 1.879(2) \AA for Si–C(1); cf. 1.881(2) and 1.884(2) \AA for **1e**) but the degree of lengthening is inversely dependent upon the length of the Si \cdots N interaction and, thus, is less than that seen for **5a**. As is seen with the structure of **5a**, **5b** has a pseudo-trigonal bipyramidal structure at the bridging silicon center, with the C_{ipso} carbon atom *trans* to the NMe_2 group (C(6)) and its nitrogen atom in the axial positions, and the remaining C_{ipso} carbon atom (C(1)) and the aryl ring and CH_2Cl groups in the equatorial positions. The C(6)–Si(1)–N(1) angle of 173.5 $^\circ$ approaches the theoretical value of 180 $^\circ$. The equatorial angles range from 110.5 $^\circ$ (C(1)–Si(1)–C(20)) to 119.8 $^\circ$ (C(11)–Si(1)–C(20)) and their sum, 345.4 $^\circ$, corresponds to a value of 53.6% pentacoordination character (% TBP $_{\text{e}}$).^[22] The α angle for the structure is larger than typical for a tetracoordinate sila[1]ferrocenophane, with a value of 21.4 $^\circ$ (cf. 20.4(1) for **1e**), and the β angles are consequently smaller with an average of 36.2 $^\circ$. As for **5a**, the Fe \cdots Si distance of 2.7402(7) \AA is longer than expected (cf. 2.6903(7) \AA for **1e**) and could be a consequence of a smaller interaction between these atoms when in proximity to the intramolecularly donating NMe_2 group.

Conversion of **5b** to the spirocyclic sila[1]ferrocenophane **9-Cl**

Although synthesis and isolation of **5b** were relatively facile, this species was found to exhibit low stability at room temperature in both solution and the solid state. Thus, a CD_2Cl_2 solution of **5b**, monitored over time by ^1H NMR spectroscopy, showed clean conversion to a new, CD_2Cl_2 -soluble, product. At room temperature, the reaction reached about 50% conversion after 10 minutes, neared completion after ~ 1 h, and complete consumption of **5b** occurred if it was left in solution for ~ 12 h; CH_2Cl_2 solutions of **5b** showed much slower reactivity when held at lower temperatures.

The ^1H NMR resonances of the new product were consistent with the formation of the internal cyclization salt [$\text{FeSi}(\text{CH}_2\text{NMe}_2\text{CH}_2\text{C}_6\text{H}_4)$] Cl^- (**9-Cl**) [Eq. (5)]. Resonances



due to **9** were readily identifiable in the spectrum acquired at 50% conversion. Further confirmation of these shifts was provided by the spectrum acquired after 12 h.^[25] The ^1H NMR spectrum of **9** showed downfield shifts of the methylene and methyl resonances of the CH_2NMe_2 arm to $\delta = 5.10$ and 3.74 ppm, respectively (cf. $\delta = 3.38$ and 1.89 ppm for **5b**), that were consistent with quaternization of the nitrogen atom. Also, the resonance due to the methylene group between the two heteroatoms of the new six-membered ring was downfield shifted ($\delta = 4.28$ ppm) relative to the CH_2Cl resonance seen for **5b** ($\delta = 3.31$ ppm). ^{13}C and ^{29}Si NMR spectra were acquired in the interval between the 1 h and 12 h points of the reaction to maximize the signals due to **9** in solution. The ^{13}C NMR spectrum supported the identification of the new

product as **9-Cl**, with signals at $\delta = 68.4$ (ArCH₂), 55.8 (Me) and 54.6 ppm (SiCH₂) that were consistent with carbon atoms bonded to a cationic nitrogen atom. The single ²⁹Si NMR resonance at $\delta = -27.1$ ppm is significantly upfield shifted from that of **5b** ($\delta = -14.8$ ppm) and is indicative of its proximity to the quaternized nitrogen center.

In the solid state, crystals of **5b** undergo an irreversible transformation over several weeks that renders them completely insoluble in many solvents in which **5b** was initially soluble (e.g. hexanes, toluene, THF). Analysis of the product by solid state CP-MAS ²⁹Si NMR showed a single new broad resonance at $\delta = -26.9$ ppm. The solid state CP-MAS ¹³C NMR spectrum was also inconsistent with the structure of **5b**. Notably, the CP-MAS spectra of the solid state conversion product (vide supra) are consistent with the ¹³C and ²⁹Si NMR spectra of **9-Cl** and indicate that reactions between the CH₂Cl functionalities of **5b** and its NMe₂ groups are involved in its solid state transformation. Elemental analysis data showed that the product possessed the same composition as **5b** and was consistent with such a rearrangement [Eq. (5)].

Confirmation of the structure of **9-Cl** was carried out by means of a single crystal X-ray diffraction study (Figure 8).

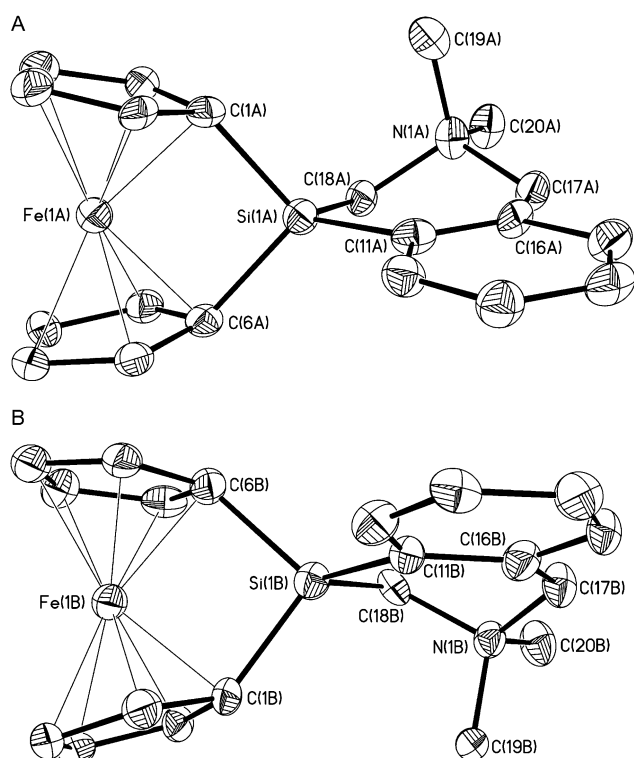


Figure 8. Molecular structures of the two independent molecules (A and B) in the unit cell of **9-Cl**·CH₂Cl₂ that show thermal ellipsoids at 30% probability.

Selected bond lengths and angles are shown in Table 6. Suitable crystals of **9-Cl**·CH₂Cl₂ were obtained after a solution of **5b** in CH₂Cl₂ was allowed to stir at room temperature for 1 h and then cooled to -30 °C overnight. The two ring conformers (A and B) of the product crystallize together in the non-centrosymmetric orthorhombic space

Table 6. Selected bond lengths [Å] and angles [°] for **9-Cl**·CH₂Cl₂.

Si(1A)–Fe(1A)	2.689(3)	Si(1B)–Fe(1B)	2.683(3)
Si(1A)–C(1A)	1.878(9)	Si(1B)–C(1B)	1.867(9)
Si(1A)–C(6A)	1.886(8)	Si(1B)–C(6B)	1.883(8)
Si(1A)–C(11A)	1.845(10)	Si(1B)–C(11B)	1.847(10)
Si(1A)–C(18A)	1.886(8)	Si(1B)–C(18B)	1.878(8)
C(1A)–Si(1A)–C(6A)	96.2(4)	C(1B)–Si(1B)–C(6B)	96.7(4)
C(1A)–Si(1A)–C(11A)	116.8(4)	C(1B)–Si(1B)–C(11B)	116.7(4)
C(1A)–Si(1A)–C(18A)	113.5(4)	C(1B)–Si(1B)–C(18B)	112.2(4)
C(6A)–Si(1A)–C(11A)	118.6(4)	C(6B)–Si(1B)–C(11B)	118.4(4)
C(6A)–Si(1A)–C(18A)	108.9(4)	C(6B)–Si(1B)–C(18B)	109.4(4)
C(11A)–Si(1A)–C(18A)	103.1(4)	C(11B)–Si(1B)–C(18B)	103.6(4)
Si(1A)–C(11A)–C(16A)	120.0(6)	Si(1B)–C(11B)–C(16B)	121.4(7)
Si(1A)–C(18A)–N(1A)	110.1(5)	Si(1B)–C(18B)–N(1B)	111.0(6)
C(11A)–C(16A)–C(17A)	126.0(8)	C(11B)–C(16B)–C(17B)	122.4(9)
N(1A)–C(17A)–C(16A)	116.9(7)	N(1B)–C(17B)–C(16B)	117.6(7)
C(17A)–N(1A)–C(18A)	110.1(7)	C(17B)–N(1B)–C(18B)	112.1(7)
C(17A)–N(1A)–C(19A)	113.3(7)	C(17B)–N(1B)–C(19B)	111.1(7)
C(17A)–N(1A)–C(20A)	106.8(7)	C(17B)–N(1B)–C(20B)	107.5(7)
C(18A)–N(1A)–C(19A)	110.0(7)	C(18B)–N(1B)–C(19B)	110.4(6)
C(18A)–N(1A)–C(20A)	109.0(6)	C(18B)–N(1B)–C(20B)	107.7(6)
C(19A)–N(1A)–C(20A)	107.6(7)	C(19B)–N(1B)–C(20B)	107.9(6)

group *P*2₁2₁ with the eight molecules of [**9**]⁺ in the unit cell showing pseudo-inversion symmetry. Both enantiomers show ring tilts ($\alpha = 20.4(3)$ and $21.1(3)^\circ$, for A and B, respectively) typical of sila[1]ferrocenophanes. The intramolecular cyclization gives rise to a spirocyclic unit centered about silicon. The endocyclic angles about silicon, for the ferrocenophane rings ($96.2(4)^\circ$ for A, $96.7(4)^\circ$ for B) as well as the SiCNC₃ rings ($103.1(4)^\circ$ for A, 103.6° for B) are significantly contracted relative to those found for an ideal tetrahedron. However, the exocyclic angles ($108.9(4)^\circ$ to $118.6(4)^\circ$) are consequently larger, with the largest corresponding to the C(6)–Si(1)–C(11) angle, and the average C–Si–C angle is 109.5° . The SiCNC₃ cycles show planarity for the four atoms (Si(1), C(11), C(16), and C(17)) adjacent to the aromatic ring. The C(18) atoms in both A and B show only slight displacement from this plane, whereas the N atoms are significantly displaced, with the planes defined by C(17)–N(1)–C(18) at 51.4° (A) and 50.2° (B) angles to the SiCCC planes. The geometry about nitrogen approaches tetrahedral with C–N–C angles ranging from $106.8(7)$ to $113.3(7)^\circ$ and averaging 109.5° . Although the synthesis of several compounds that incorporate the cationic SiCNC₃ ring structure have been previously reported,^[26] none of these reports include characterization by X-ray crystallography.

Quaternization of [fcSi(CH₂Cl)(2-C₆H₄CH₂NMe₂)] (5b): As with the case of **5a** we found that it was possible to quaternize the NMe₂ group of **5b** through reaction with MeOTf at 0 °C [Eq. (4)]. The increased reactivity of **5b** in solution (over that of **5a**), as indicated by the VT-NMR data, as well as its tendency towards intramolecular cyclization at room temperature, leads to side reactions and makes isolation of pure [fcSi(CH₂Cl)(2-C₆H₄CH₂NMe₃)]⁺[OTf][−] (**7b-OTf**) difficult. However, **7b-OTf** can be isolated in low yields by means of repeated recrystallizations from a 2:1 mixture of CH₂Cl₂/hexanes.

Unlike **7a-OTf**, this species is insoluble in C₆D₆ and a more polar solvent, such as CD₂Cl₂, is required for solution NMR

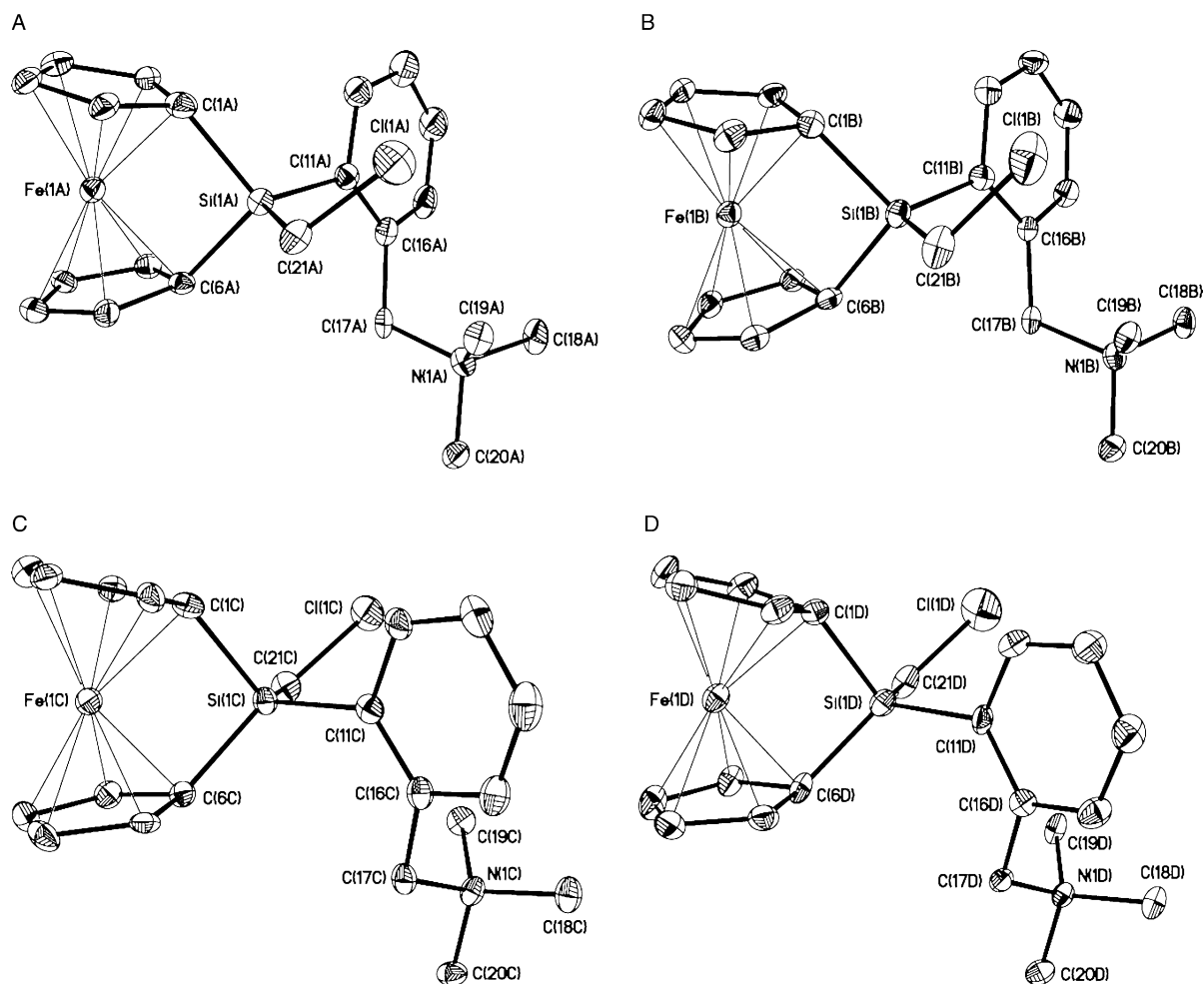
studies. However, as seen for **7a**, down-field shifts of the methyl and methylene proton resonances of the quaternized arm, from $\delta = 1.89$ and 3.38 ppm (**5b** in C_6D_6) to $\delta = 3.24$ and 5.12 ppm (CD_2Cl_2), respectively, are indicative of the quaternization of the nitrogen atom. ^{13}C NMR spectroscopy further confirms the identity of **7b** in solution. As seen in the case of **7a** the ^{29}Si NMR signal for **7b** ($\delta = -10.9$ ppm) is downfield from that seen for the unquaternized **5b** ($\delta = -14.8$ ppm) and approaches that seen for the non-hypercoordinate analogue **1e** ($\delta = -10.4$ ppm).

In order to further characterize **7b**-OTf an X-ray diffraction study was performed on single crystals obtained from CH_2Cl_2 . Compound **7b**-OTf $\cdot CH_2Cl_2$ was found to crystallize in the space group Cc with four independent molecules (A–D) in the asymmetric unit (Figure 9, Table 7). Each of these molecules showed structural similarities to the methyl-substituted analogue **7a**-OTf. Again, quaternization of the nitrogen atom results in the $CH_2NMe_3^+$ moiety bending away from the silicon, with Si(1)-C(11)-C(16) angles wider than the expected trigonal angle (from $125.3(5)$ to $127.6(5)^\circ$). The nitrogen centers show tetrahedral geometry, with an average C-N-C angle of 109.5° . The silicon centers once again approach tetrahedral, rather than trigonal bipyramidal, environments (average C-Si-C angles of 109.1 to 109.2°) and the

Table 7. Selected bond lengths [\AA] and angles [$^\circ$] for **7b**-OTf $\cdot CH_2Cl_2$.

Molecule	A	B	C	D
Si(1)–Fe(1)	2.669(2)	2.678(2)	2.679(2)	2.692(2)
Si(1)–C(1)	1.889(8)	1.880(7)	1.870(7)	1.867(7)
Si(1)–C(6)	1.888(7)	1.859(7)	1.866(7)	1.871(7)
Si(1)–C(11)	1.875(7)	1.886(6)	1.868(7)	1.886(7)
Si(1)–C(21)	1.888(7)	1.862(7)	1.866(7)	1.850(7)
C(1)–Si(1)–C(6)	97.2(3)	98.0(3)	96.7(3)	96.8(3)
C(1)–Si(1)–C(11)	109.4(3)	109.5(3)	109.9(3)	109.1(3)
C(1)–Si(1)–C(21)	108.8(3)	107.7(3)	108.6(3)	109.1(3)
C(6)–Si(1)–C(11)	113.4(3)	112.1(3)	113.6(3)	113.7(3)
C(6)–Si(1)–C(21)	108.7(3)	110.8(3)	109.6(3)	111.6(3)
C(11)–Si(1)–C(21)	117.3(3)	116.9(3)	116.5(3)	114.9(3)
Si(1)–C(11)–C(16)	127.6(5)	126.7(5)	126.8(5)	125.3(5)
C(11)–C(16)–C(17)	121.6(6)	122.7(5)	122.5(6)	124.3(6)
N(1)–C(17)–C(16)	114.2(5)	114.6(5)	114.2(5)	114.8(5)
C(17)–N(1)–C(18)	112.0(5)	111.2(5)	112.8(5)	111.5(5)
C(17)–N(1)–C(19)	110.7(5)	110.0(5)	110.0(5)	110.4(5)
C(17)–N(1)–C(20)	108.4(5)	107.8(5)	107.7(5)	107.8(5)
C(18)–N(1)–C(19)	108.7(5)	109.6(5)	109.5(5)	109.3(5)
C(18)–N(1)–C(20)	107.6(5)	108.3(5)	108.4(5)	107.7(5)
C(19)–N(1)–C(20)	109.5(5)	109.9(5)	108.4(5)	110.0(5)

endocyclic C(1)–Si(1)–C(6) angles of 96.7 to 98.0° represent, as expected, the largest deviations from ideal tetrahedral geometry. The tilt angles (α) of $19.97(15)$, $20.13(17)$,

Figure 9. Molecular structures of the four independent molecules (A–D) in the unit cell of **7b** that show thermal ellipsoids at 30% probability.

20.59(17) and 20.60(18)° between the planes of the Cp rings are typical for silicon-bridged ferrocenophanes.^[3]

Conclusion

We have demonstrated the synthesis of the first pentacoordinate sila[1]ferrocenophanes **5a** and **5b** and investigated their fluxionality, reactivity and structure. The susceptibility of these species to quaternization by methyl triflate is suggestive that the source of their fluxionality is the fast, reversible coordination of the NMe₂ group to the silicon center. Such fluxionality is consistent with the results of variable-temperature NMR studies of **5a** and **5b** in solution. In addition, **5b** was shown to undergo an unprecedented intramolecular cyclization reaction to yield the spirocyclic salt **9-Cl**. Single-crystal X-ray diffraction studies have demonstrated that **5a** and **5b** may function as models of intermediates or transition states in the nucleophilically-assisted as well as the thermal ring-opening polymerizations of Group 14 bridged [1]ferrocenophanes. Further studies to probe this possibility will be the subject of future work.

Experimental Section

General procedures: C₆H₅CH₂NMe₂, *n*BuLi (1.6 M in hexanes), PhLi (1.8 M in cyclohexane), and MeOTf were purchased from Aldrich and were used without further purification. Me₃SiCl was purchased from Aldrich and distilled prior to use. 2-Li[C₆H₄CH₂NMe₂] was prepared from C₆H₅CH₂NMe₂ and *n*BuLi (1.6 M in hexanes) in Et₂O.^[27] Dilithioferrocene·*n*TMEDA,^[28] [fcSiMeCl] (**1a**),^[29] [fcSiMePh] (**1b**)^[14] and [fcSiCl₂] (**1c**)^[8b] were synthesized according to literature procedures. All reactions and manipulations were carried out under an atmosphere of pre-purified nitrogen using either Schlenk techniques or an inert atmosphere glove box. Solvents were dried using the Grubbs method or by standard methods followed by distillation.

¹H (300 or 400 MHz) and ¹³C NMR (75.5 or 100.4 MHz) spectra were recorded on either Varian Gemini300 or Varian Unity400 spectrometers and were referenced internally to protonated solvent shifts. All ¹³C NMR spectra were obtained using proton decoupling. ²⁹Si NMR spectra (Varian Unity400 in DEPT mode at 79.3 MHz) and ¹⁹F NMR spectra (Varian Gemini300 at 282.3 MHz) were referenced externally to SiMe₄ and CFCl₃ in CDCl₃, respectively. Solid-state CP-MAS ¹³C and ²⁹Si spectra were obtained on a Bruker DSSX400 instrument with a spin rate of 9 KHz.

Mass spectra were obtained with the use of a VG 70-250S mass spectrometer operating in Electron Impact (EI) mode. Pyrolysis mass spectra are reported for maximum ion output. UV/Vis spectra were acquired using a Perkin Elmer Lambda 900 UV/Vis/NIR spectrometer on 10⁻³ M solution in CH₂Cl₂.

Synthesis of [fcSiMe(2-C₆H₄CH₂NMe₂)] (5a**):** A solution of Li[2-C₆H₄CH₂NMe₂] (0.59 g, 4.19 mmol) in THF (15 mL) was cooled to -78 °C and slowly added to a solution of **1a** (1.00 g, 3.81 mmol) in THF (30 mL) at -78 °C. The reaction mixture was slowly warmed to -30 °C and Me₃SiCl (0.1 mL) was added with a syringe. After the mixture had been warmed to room temperature, all volatile material was removed under vacuum (12 h at room temperature). Recrystallization from hexanes (15 mL) at -30 °C gave dark red crystals of **5a** (0.70 g, 51 %) suitable for single-crystal X-ray diffraction. A second fraction (0.42 g) was obtained after concentration of the filtrate to 3 mL to give an overall yield of 81 %. ¹H NMR (400 MHz, C₆D₆, 20 °C): δ = 8.29 (m, 1H; Ph-H6), 7.22–7.10 (m, 3H; Ph-H3–5), 4.45 (m, 2H; Cp), 4.38 (m, 2H; Cp), 4.15 (m, 2H; Cp), 3.89 (m, 2H; Cp), 3.50 (s, 2H; CH₂), 1.97 (s, 6H; NCH₃), 0.70 ppm (s, 3H; SiCH₃); ¹³C NMR (100.5 MHz, C₆D₆, 20 °C): δ = 147.5 (*ipso*-Ph), 137.0 (Ph), 135.1 (*ipso*-Ph), 129.9 (Ph), 128.5 (Ph), 127.0 (Ph), 77.1 (Cp), 77.0 (Cp), 76.1

(Cp), 75.5 (Cp), 64.3 (CH₂), 44.5 (NCH₃), 37.4 (*ipso*-Cp), -2.1 ppm (SiCH₃); ²⁹Si NMR (79.3 MHz, C₆D₆, 20 °C): δ = -13.9 ppm; ²⁹Si CP-MAS NMR (79.5 MHz, 20 °C): δ = -12.8 ppm; MS (70 eV, EI): *m/z* (%): 361 (42) [*M*⁺], 346 (100) [*M*⁺ - CH₃], 317 (27) [*M*⁺ - N(CH₃)₂]; UV/Vis (10⁻³ M in CH₂Cl₂): λ_{max} (log ε) = 482 nm (276 m⁻¹cm⁻¹); elemental analysis calcd (%) for C₂₀H₂₃FeNSi (361.34): C 66.48, H 6.42, N 3.88; found: C 66.51, H 6.47, N 3.76.

Synthesis of [fcSiMe(2-C₆H₄CH₂NMe₃)](OTf) (7a-OTf**):** MeOTf (0.228 g, 1.39 mmol) dissolved in toluene (2 mL) was added dropwise to a solution of **5a** (0.497 g, 1.38 mmol) in toluene (50 mL) at 0 °C, slowly warmed to room temperature and reacted for 18 h. All volatile material was removed under vacuum (12 h at 25 °C). Recrystallization from CH₂Cl₂/hexanes at -20 °C gave red crystals of **7a-OTf**·CH₂Cl₂ (0.683 g, 81 %). ¹H NMR (300 MHz, C₆D₆, 20 °C): δ = 7.93 (d, ³J(H,H) = 7.5 Hz, 1H; Ph-H3), 7.84 (d, ³J(H,H) = 7.7 Hz, 1H; Ph-H6), 7.32 (t, 1H; Ph-H4), 7.18 (t, 1H; Ph-H5), 4.91 (s, 2H; CH₂), 4.36 (s, 2H; Cp), 4.29 (m, 4H; Cp; CH₂Cl₂), 4.01 (s, 2H; Cp), 3.47 (s, 2H; Cp), 2.83 (s, 9H; NCH₃), 0.43 ppm (s, 3H; SiCH₃); ¹³C NMR (75.5 MHz, C₆D₆, 20 °C): δ = 138.5 (*ipso*-Ph), 136.6 (Ph), 135.2 (Ph), 134.0 (*ipso*-Ph), 130.9 (Ph), 130.0 (Ph), 122.2 (q, ¹J(C,F) = 321 Hz, CF₃), 78.6 (Cp), 78.5 (Cp), 76.5 (Cp), 76.1 (Cp), 68.3 (CH₂), 52.5 (NCH₃), 31.9 (*ipso*-Cp), -2.5 ppm (SiCH₃); ¹⁹F NMR (282.3 MHz, C₆D₆, 20 °C): δ = -78.1 ppm; ²⁹Si NMR (79.3 MHz, C₆D₆, 20 °C): δ = -9.2 ppm; UV/Vis (10⁻³ M in CH₂Cl₂): λ_{max} (log ε) = 487 nm (305 m⁻¹cm⁻¹); elemental analysis calcd (%) for C₂₂H₂₆F₃FeNO₃SSi·0.3CH₂Cl₂ (550.93): C 48.62, H 4.87; found C 48.39 H 4.82; the amount of CH₂Cl₂ in the sample, that was not removed after 24 h under high vacuum, was estimated by ¹H NMR spectroscopy.

Synthesis of [FcSi(2-C₆H₄CH₂NMe₂)] (8**):** A solution of Li[2-C₆H₄CH₂NMe₂] (0.61 g, 4.32 mmol) in THF (25 mL) was added dropwise to a solution of [Fc₂SiCl₂] (2.00 g, 4.26 mmol) in THF (50 mL) cooled to -78 °C. The solution was allowed to warm slowly to room temperature and the solvent removed. ¹H NMR spectra showed 60 % conversion to the disubstituted product and the mixture was redissolved in THF and a further 0.40 g solution of Li[2-C₆H₄CH₂NMe₂] in THF was added to complete conversion to **8**. The product was recrystallized from Et₂O/hexanes at -50 °C to yield dark red crystals (0.752 g, 27 %). ¹H NMR (300 MHz, C₆D₆, 25 °C): δ = 7.96 (pd, 2H; Ph), 7.86 (pd, 2H; Ph), 7.28 (pt, 2H; Ph), 7.07 (pt, 2H; Ph), 4.60 (pt, 4H; Cp), 4.34 (pt, 4H; Cp) 3.93 (s, 10H; Cp), 3.58 (s, 4H; CH₂), 2.03 ppm (s, 12H; NCH₃); ¹³C NMR (300 MHz, C₆D₆, 25 °C): δ = 150.4 (*ipso*-Ph), 146.0 (Ph), 138.0 (*ipso*-Ph), 137.6 (Ph), 130.0 (Ph), 129.4 (Ph), 126.4 (Ph), 76.7 (Cp), 71.8 (Cp), 70.3 (*ipso*-Cp), 69.7 (CH₂), 45.8 ppm (NCH₃); ²⁹Si (79.5 MHz, C₆D₆): δ = -13.0 ppm; ¹H NMR (400 MHz, CD₂Cl₂, 25 °C): δ = 7.74 (pd, 2H; Ph), 7.62 (pd, 2H; Ph), 7.40 (pt, 2H; Ph), 7.22 (pt, 2H; Ph), 4.49 (pt, 4H; Cp), 4.48 (pt, 4H; Cp) 3.91 (s, 10H; Cp), 3.39 (s, 4H; CH₂), 1.99 ppm (s, 12H; NCH₃); ¹³C NMR (400 MHz, CD₂Cl₂, 25 °C): δ = 145.6 (*ipso*-Ph), 137.7 (*ipso*-Ph), 137.3 (Ph), 129.6 (Ph), 128.9 (Ph), 126.1 (Ph), 76.5 (Cp), 71.6 (Cp), 69.9 (*ipso*-Cp), 69.4 (CH₂), 45.6 ppm (NCH₃); ²⁹Si (79.5 MHz, CD₂Cl₂): δ = -13.6 ppm; elemental analysis calcd (%) for C₃₈H₄₂Fe₂N₂Si (666.54): C 68.48, H 6.35, N 4.20; found C 68.38, H 6.41, N 4.26.

Attempted synthesis of [fcSiCl(2-C₆H₄CH₂NMe₂)]: A solution of Li[2-C₆H₄CH₂NMe₂] (0.245 g, 1.74 mmol) in THF (100 mL) was cooled to -78 °C and transferred with a cannula into a solution of **1c** (0.499 g, 1.76 mmol) in THF (100 mL) at -78 °C. The solution was warmed slowly to -30 °C, stirred for 1 h and then warmed to room temperature. The solvent was removed, the product redissolved in toluene and filtered to remove LiCl. ¹H, ¹³C, and ²⁹Si NMR spectra showed a complex mixture of products. ²⁹Si NMR (79 MHz, C₆D₆, 25 °C): δ = -5.26 (major), -18.13 (major), -21.76 (minor), -28.04 (major), -29.33 (minor), -31.63 (minor), -36.25 ppm (minor). Further, treatment of this reaction mixture with MeLi led to a mixture of products that we were unable to characterize further.

Synthesis of [fcSi(CH₂Cl)Cl] (1d**):** (ClCH₂)₂SiCl₃ (7.350 g, 39.95 mmol) was added dropwise to a suspension of [fLi₂]·³/TMEDA (10.013 g, 36.15 mmol) in Et₂O (350 mL) at -78 °C. The suspension was warmed slowly (~2 h) to room temperature and the solvent, excess silane and TMEDA were removed under reduced pressure. Hexanes were added to redissolve the desired product and the solution was filtered to remove LiCl. The product was isolated as red needles by recrystallization from hexanes at -50 °C (7.299 g, 68 %). ¹H NMR (400 MHz, C₆D₆, 25 °C): δ = 4.29 (pt, 4H; Cp), 4.11 (pq, 2H; Cp) 3.94 (pq, 2H; Cp), 2.83 ppm (s, 2H; CH₂);

^{13}C NMR (100 MHz, C_6D_6 , 25 °C): $\delta = 79.1$ (Cp), 79.0 (Cp), 75.9 (Cp), 74.6 (Cp), 31.4 (*ipso*-Cp), 28.1 ppm (CH_2); ^{29}Si NMR (79 MHz, C_6D_6 , 25 °C): $\delta = -0.34$ ppm; MS (70 eV, EI): *m/z* (%): 296 (100) [M^+], 247 (5) [$M^+ - \text{CH}_2\text{Cl}$], 183 (12) [$M^+ - \text{CH}_2\text{Cl} - \text{C}_5\text{H}_4$]; high-resolution MS for $\text{C}_{11}\text{H}_{10}\text{Cl}_2\text{FeSi}$: calcd 295.928; found 295.953.

Synthesis of [fcSi(CH₂Cl)(2-C₆H₄CH₂NMe₂)] (5b): A solution of Li[2-C₆H₄CH₂NMe₂] (0.657 g, 4.66 mmol) in THF (50 mL) was cooled to -78°C and slowly added to a solution of **1d** (1.263 g, 4.25 mmol) in THF (50 mL) at -78°C . The reaction mixture was slowly warmed to -30°C and Me_3SiCl (0.13 mL) was added with a syringe. After the mixture had been warmed to room temperature, all volatile material was removed under vacuum (12 h at room temperature). The product was redissolved in hexanes and filtered to remove LiCl. Recrystallization from hexanes at -20°C gave dark red crystals of **5b** (1.118 g, 66%) suitable for single-crystal X-ray diffraction. ^1H NMR (400 MHz, C_6D_6 , 25 °C): $\delta = 8.29$ (m, 1H; Ph-H6), 7.19–7.01 (m, 3H; Ph-H3–5), 4.40 (m, 2H; Cp), 4.31 (m, 2H; Cp), 4.23 (m, 2H; Cp), 3.79 (m, 2H; Cp), 3.38 (brs, 2H; CH₂), 3.31 (s, 2H; CH₂Cl), 1.89 ppm (s, 6H; NCH₃); ^{13}C NMR (100.5 MHz, C_6D_6 , 20 °C): $\delta = 147.6$ (*ipso*-Ph), 138.5 (Ph), 131.4 (*ipso*-Ph), 130.4 (Ph), 128.7 (Ph), 127.0 (Ph), 77.7 (Cp), 77.1 (Cp), 76.0 (Cp), 75.6 (Cp), 64.3 (CH₂), 44.5 (NCH₃), 35.2 (*ipso*-Cp), 29.1 ppm (SiCH₂); ^{29}Si NMR (79.3 MHz, C_6D_6 , 20 °C) $\delta = -14.8$ ppm; elemental analysis calcd (%) for $\text{C}_{20}\text{H}_{22}\text{ClFeNSi}$ (395.79): C 60.69, H 5.60, N 3.54; found C 60.79, H 5.30, N 3.17.

Synthesis of [fcSi(CH₂Cl)Ph] (1e): A solution of PhLi (1.03 mL, 1.8 M in cyclohexane, 1.85 mmol) was slowly injected into a solution of **1d** (0.500 g, 1.68 mmol) in THF (20 mL) at -78°C . The reaction mixture was slowly warmed to -20°C and Me_3SiCl (0.1 mL) was added with a syringe. After warming to room temperature all volatile material was removed under vacuum (12 h at room temperature) and the product was recrystallized from hexanes at -20°C to give **1e** (0.202 g, 36%). ^1H NMR (400 MHz, C_6D_6 , 25 °C): $\delta = 7.94$ (m, 2H; Ph), 7.25 (d, 2H; Ph), 7.24 (m, 1H; Ph), 4.40 (m, 2H; Cp), 4.31 (m, 2H; Cp), 4.09 (m, 2H; Cp), 3.87 (m, 2H; Cp), 2.99 ppm (s, 2H; CH₂Cl); ^{13}C NMR (100.5 MHz, C_6D_6 , 20 °C): $\delta = 135.2$ (Ph), 131.9 (*ipso*-Ph), 131.2 (Ph), 128.5 (Ph), 78.6 (Cp), 78.1 (Cp), 76.6 (Cp), 76.1 (Cp), 30.0 (*ipso*-Cp), 27.4 ppm (CH₂Cl); ^{29}Si NMR (79.3 MHz, C_6D_6 , 20 °C): $\delta = -10.4$ ppm; MS (70 eV, EI): *m/z* (%): 338 (100) [M^+], 289 (15) [$M^+ - \text{CH}_2\text{Cl}$], 169 (17) [$M^+ - \text{CH}_2\text{Cl} - \text{C}_5\text{H}_4 - \text{Fe}$], 105 (11) [SiC_6H_5^+]; high-resolution MS for $\text{C}_{17}\text{H}_{15}\text{ClFeSi}$: calcd 337.998; found 337.998.

Conversion of 5b to 9-Cl monitored by NMR spectroscopy: The conversion of **5b** (0.020 g) to **9-Cl** at room temperature in CD_2Cl_2 (0.75 mL) was monitored by ^1H NMR spectroscopy. The reaction reached 50% conversion after 10 min, ~95% conversion after 1 h and complete conversion between 1–12 h.^[25] For **9-Cl**: ^1H NMR (400 MHz, CD_2Cl_2 , 25 °C): $\delta = 8.00$ (m, 1H; Ph), 7.61 (m, 2H; Ph), 7.51 (m, 1H; Ph), 5.10 (s, 2H; NCH₂Ph), 4.70 (m, 2H; Cp), 4.65 (m, 2H; Cp), 4.51 (m, 2H; Cp), 4.46 (m, 2H; Cp), 4.28 (s, 2H; SiCH₂N), 3.74 ppm (s, 6H; NMe₂); ^{13}C NMR (100.5 MHz, CD_2Cl_2 , 25 °C): $\delta = 136.0$ (*ipso*-Ph), 135.2 (Ph), 132.1 (Ph), 130.1 (Ph), 129.4 (Ph), 127.4 (*ipso*-Ph), 79.5 (Cp), 79.2 (Cp), 75.5 (Cp), 74.9 (Cp), 68.4 (ArCH₂N), 55.8 (NMe₂), 54.6 (SiCH₂N), 24.7 ppm (*ipso*-Cp); ^{29}Si NMR (79.3 MHz, CD_2Cl_2 , 25 °C): $\delta = -27.1$ ppm.

Isolation of X-ray diffraction quality crystals of [fcSi(c-C₆H₄CH₂NMe₂-

CH₂Cl)] (9-Cl): Crystals of **5b** (0.197 g, 0.498 mmol) were dissolved in ~20 mL of CH_2Cl_2 and left under N_2 at room temperature for approximately 1 h. Crystals of **9-Cl**· CH_2Cl_2 suitable for X-ray diffraction were isolated by crystallization at -30°C (0.098 g, 41%).

Solid state conversion of 5b into 9-Cl: Crystals of **5b** were left at room temperature over ~5 months, after which they no longer diffracted X-rays or showed significant solubility in hexanes, toluene, or tetrahydrofuran. ^{13}C CP-MAS NMR (100.6 MHz, $k = 9$ kHz, 27 °C): $\delta = 130.2$ (Ph), 77.2 (Cp), 69.8 (PhCH₂N), 59.0 (NCH₃), 51.6 (SiCH₂N), 26.7 ppm (*ipso*-Cp); ^{29}Si CP-MAS NMR (79.5 MHz, $k = 9$ kHz, 27 °C): $\delta = -26.9$ ppm; elemental analysis calcd (%) for $\text{C}_{20}\text{H}_{22}\text{ClFeNSi}$ (395.79): C 60.69, H 5.60, N 3.54; found C 60.30, H 5.73, N 3.31.

Synthesis of [fcSi(CH₂Cl)(2-C₆H₄CH₂NMe₂)] [OTf] (7b-OTf): MeOTf (0.083 g, 0.51 mmol) was added dropwise to a solution of **5b** (0.200 g, 0.505 mmol) in toluene (20 mL) at 0 °C and slowly warmed to room temperature. All volatile material was removed under vacuum and recrystallization from CH_2Cl_2 /hexanes at -30°C gave red crystals of **7b-OTf**· CH_2Cl_2 (0.153 g, 47%). ^1H NMR (400 MHz, CD_2Cl_2 , 25 °C): $\delta = 8.30$ (dd, $^3J(\text{H,H}) = 7.2$ Hz, $^4J(\text{H,H}) = 1.6$ Hz, 1H; *o*-Ph), 7.84 (d, $^3J(\text{H,H}) = 7.6$ Hz, 1H; Ph) 7.73 (m, 2H; Ph), 5.33 (CH₂Cl₂), 5.12 (m, 2H; CH₂), 4.68 (m, 2H; Cp), 4.63 (m, 2H; Cp), 4.38 (m, 2H; Cp), 3.94 (m, 2H; Cp), 3.45 (s, 2H; CH₂Cl), 3.24 ppm (s, 9H; NCH₃); ^{13}C NMR (100 MHz, C_6D_6 , 20 °C): $\delta = 139.0$ (Ph), 135.2 (*ipso*-Ph), 134.7 (Ph), 134.3 (*ipso*-Ph), 132.0 (Ph), 130.7 (Ph), 122.8 (q, $^1J(\text{C,F}) = 632$ Hz; CF₃), 79.7 (Cp), 79.2 (Cp), 76.5 (Cp), 76.3 (Cp), 69.3 (CH₂), 53.9 (NCH₃), 29.4 (*ipso*-Cp), 27.4 ppm (SiCH₂Cl); ^{19}F NMR (282.3 MHz, C_6D_6 , 20 °C): $\delta = -78.5$ ppm; ^{29}Si NMR (79.3 MHz, C_6D_6 , 20 °C): $\delta = -10.9$ ppm.

Variable-temperature NMR spectroscopy: All compounds were dissolved in a suitable deuterated solvent (CD_2Cl_2 or $[\text{D}_8]\text{toluene}$) and rapidly placed

Table 8. Crystallographic data for **5a**, **7a-OTf**· CH_2Cl_2 , and **8**.

	5a	7a-OTf · CH_2Cl_2	8
empirical formula	$\text{C}_{20}\text{H}_{23}\text{FeNSi}$	$\text{C}_{23}\text{H}_{28}\text{Cl}_2\text{F}_3\text{FeNO}_3\text{SSi}$	$\text{C}_{38}\text{H}_{42}\text{Fe}_2\text{N}_2\text{Si}$
fw	361.33	610.36	666.53
crystal color, habit	orange-red, block	orange, block	orange-red, block
temperature [K]	100.0(1)	173(2)	150(1)
wavelength [Å]	0.71073	0.71073	0.71073
crystal system	monoclinic	orthorhombic	triclinic
space group	$P2_1/n$	$Pna2_1$	$P\bar{1}$
<i>a</i> [Å]	7.5146(2)	19.7588(2)	9.2811(2)
<i>b</i> [Å]	12.8744(4)	15.6016(2)	9.8634(3)
<i>c</i> [Å]	18.0268(5)	8.4520(2)	19.7028(6)
α [°]	90	90	80.391(2)
β [°]	97.010(16)	90	77.161(2)
γ [°]	90	90	65.544(2)
volume [Å ³]	1730.98(9)	2605.48(6)	1595.07(8)
<i>Z</i>	4	4	2
ρ_{calcd} [g cm ⁻³]	1.387	1.556	1.388
μ [mm ⁻¹]	0.939	0.958	0.977
<i>F</i> (000)	760	1256	700
crystal size [mm]	0.30 × 0.22 × 0.20	0.30 × 0.25 × 0.20	0.30 × 0.30 × 0.28
θ range for data collection [°]	2.83 < θ < 27.49	2.06 < θ < 26.00	2.83 < θ < 27.51
limiting indices	0 ≤ <i>h</i> ≤ 9 0 ≤ <i>k</i> ≤ 16 -23 ≤ <i>l</i> ≤ 23	-24 ≤ <i>h</i> ≤ 23 -18 ≤ <i>k</i> ≤ 18 -10 ≤ <i>l</i> ≤ 10	0 ≤ <i>h</i> ≤ 12 -11 ≤ <i>k</i> ≤ 12 -24 ≤ <i>l</i> ≤ 25
reflections collected	12818	10855	18151
independent reflections	3964 ($R_{\text{int}} = 0.055$)	4691 ($R_{\text{int}} = 0.0362$)	7273 ($R_{\text{int}} = 0.038$)
data/restraints/parameters	3964/0/211	4691/1/316	7273/0/393
goodness of fit on F^2	0.986	1.125	1.032
final <i>R</i> indices [$I > 2\sigma(I)$]			
<i>R</i> 1	0.0352	0.0405	0.0360
<i>wR</i> 2	0.0827	0.0884	0.0841
<i>R</i> indices (all data)			
<i>R</i> 1	0.0588	0.0482	0.0521
<i>wR</i> 2	0.0885	0.0959	0.0911
extinction coefficient			0.0020(7)
largest diff peak/hole [$\text{e} \text{Å}^{-3}$]	0.348/ -0.354	0.395/ -0.311	0.393/ -0.456

in the precooled spectrometer cavity. Care was taken to avoid prolonged exposure of the solutions to room temperature environments, particularly in the case of CD_2Cl_2 solutions of **5b**. Spectra were acquired as the spectrometer was raised from temperatures near the freezing point of the chosen solvent to room temperature. Free activation energies were calculated according to: $\Delta G^\ddagger = RT_c(2.296 + \ln(T_c/\delta\nu))$ where T_c is the coalescence temperature (K) of the signals in question and $\delta\nu$ is the frequency difference (Hz) between the static signals.^[16] Temperatures were achieved through use of a heat exchange N_2 dewar and calibrated externally using a methanol standard.

For **5a**: ^1H NMR (400 MHz, CD_2Cl_2): $\delta(\text{T}) = 4.00/2.92$ (-106 , $^2J(\text{H,H}) = 12.6$ Hz; CH_2 , coal. -69 ± 5), $2.19/1.87$ ppm (-106°C ; NMe_2 , coal. $-92 \pm 1^\circ\text{C}$); ^1H NMR (400 MHz, $[\text{D}_8]\text{toluene}$): $\delta(\text{T}) = 4.39/2.56$ (-100 , CH_2 ; coal. ~ -58), $2.10/1.76$ ppm (-100°C ; NMe_2 , coal. $-88 \pm 1^\circ\text{C}$); ^{29}Si NMR (400 MHz, $[\text{D}_8]\text{toluene}$): $\delta(\text{T}) = -13.4$ (80), -13.8 (25), -15.6 ppm (-80°C).

For **5b**: ^1H NMR (300 MHz, CD_2Cl_2): $\delta(\text{T}) = 4.05/2.90$ (-96 , $^2J(\text{H,H}) = 12.9$ Hz; CH_2 , coal. -45 ± 3), $3.40/3.26$ (-96°C , $^2J(\text{H,H}) = 12.6$ Hz; CH_2Cl , coal. -60 ± 5), $2.18/1.94$ ppm (-96°C ; NMe_2 , coal. $-84 \pm 1^\circ\text{C}$); ^1H NMR (400 MHz, $[\text{D}_8]\text{toluene}$): $\delta(\text{T}) = 4.39/2.56$ (-80 , $^2J(\text{H,H}) = 12.6$ Hz; CH_2 , coal. ~ -25), $1.97/1.74$ ppm (-96°C ; NMe_2 , coal. $-78 \pm 1^\circ\text{C}$).

For **8**: ^1H NMR (400 MHz, CD_2Cl_2): Only broadening and no decoalescence of signals was observed between -80°C and room temperature.

X-Ray crystallography: Selected crystal, data collection, and refinement parameters for **1e**, **5a**, **5b**, **7a-OTf**· CH_2Cl_2 , **7b-OTf**· CH_2Cl_2 , **8**, and **9-Cl**· CH_2Cl_2 are given in Tables 8 and 9. Selected bond lengths and angles are given in Tables 1 (**5a**), 2 (**7a-OTf**· CH_2Cl_2), 3 (**8**), 4 (**5b**), 5 (**1e**), 6 (**9-Cl**· CH_2Cl_2) and 7 (**7b-OTf**· CH_2Cl_2).

For **1e**, **5a**, **5b**, **7b-OTf**· CH_2Cl_2 , **8** and **9-Cl**· CH_2Cl_2 : Single-crystal X-ray diffraction data were collected at low temperature under nitrogen with a Nonius Kappa-CCD diffractometer using graphite monochromated $\text{Mo}_{\text{K}\alpha}$ radiation ($\lambda = 0.71073$ Å). The data were integrated and scaled using the Denzo-SMN package.^[30] The SHELXTL/PC package was used to solve and refine the structures.^[31] Refinement was by full-matrix least-squares on F^2 using all data (negative intensities included). Refinement was optimized with hydrogen atoms in calculated positions. The weighting schemes were $w = 1/[\sigma^2(F_o^2) + (0.0294P)^2 + 1.1135P]$ for **1e**, $w = 1/[\sigma^2(F_o^2) + (0.0489P)^2]$ for **5a**, $w = 1/[\sigma^2(F_o^2) + (0.0326P)^2 + 2.8190P]$ for **5b**, $w = 1/[\sigma^2(F_o^2) + (0.0773P)^2 + 25.3865P]$ for **7b-OTf**· CH_2Cl_2 , $w = 1/[\sigma^2(F_o^2) + (0.0332P)^2 + 0.6588P]$ for **8** and $w = 1/[\sigma^2(F_o^2) + (0.0983P)^2]$ for **9-Cl**· CH_2Cl_2 where $P = (F_o^2 + 2F_c^2)/3$.

For **7a-OTf**· CH_2Cl_2 : Single-crystal X-ray diffraction data were collected at low temperature on a Siemens P4 diffractometer with a smart CCD detector using graphite monochromated $\text{Mo}_{\text{K}\alpha}$ radiation ($\lambda = 0.71073$ Å). The data frames were integrated and scaled using the Bruker routines SAINT and SADABS. The SHELXTL/PC package was used to solve and refine the structures.^[31] Refinement was by full-matrix least-squares on F^2 using all data (negative intensities included). Refinement was optimized with hydrogen atoms in calculated positions. The weighting scheme was $w = 1/[\sigma^2(F_o^2) + (0.0270P)^2 + 4.1260P]$ where $P = (F_o^2 + 2F_c^2)/3$.

CCDC-200059 (**1e**), CCDC-200197 (**5a**), CCDC-200054 (**5b**), CCDC-200055 (**7a-OTf**· CH_2Cl_2), CCDC-200056 (**7b-OTf**· CH_2Cl_2), CCDC-200057 (**8**) and CCDC-200058 (**9-Cl**· CH_2Cl_2) contain the supplementary crystallographic data for this paper. These data can be obtained free of charge from www.ccdc.cam.ac.uk/conts/retrieving.html (or from the Cambridge Crystallographic Data Centre, 12 Union Road, Cambridge CB21EZ, UK; fax: (+44) 1223-336-033; or e-mail: deposit@ccdc.cam.ac.uk).

Acknowledgements

Table 9. Crystallographic data for **1e**, **5b**, **7b-OTf**· CH_2Cl_2 , and **9-Cl**· CH_2Cl_2 .

	1e	5b	7b-OTf · CH_2Cl_2	9-Cl · CH_2Cl_2
empirical formula	$\text{C}_{17}\text{H}_{15}\text{ClFeSi}$	$\text{C}_{20}\text{H}_{22}\text{ClFeNSi}$	$\text{C}_{23}\text{H}_{27}\text{Cl}_3\text{F}_3\text{FeNO}_3\text{SSi}$	$\text{C}_{21}\text{H}_{24}\text{Cl}_3\text{FeNSi}$
fw	338.68	395.78	644.81	480.70
crystal color, habit	orange, plate	red, plate	orange, block	orange, plate
temperature [K]	150(1)	150(1)	150(1)	150(1)
wavelength [Å]	0.71073	0.71073	0.71073	0.71073
crystal system	monoclinic	monoclinic	monoclinic	orthorhombic
space group	$P2_1/n$	$C2/c$	Cc	$P2_12_12_1$
a [Å]	18.3960(4)	37.3913(9)	19.0710(3)	11.1010(6)
b [Å]	7.3780(4)	8.0898(2)	19.0070(4)	12.8671(8)
c [Å]	10.8650(8)	12.6531(4)	30.5980(6)	29.760(2)
α [°]	90	90	90	90
β [°]	97.833(2)	108.900(1)	100.4110(9)	90
γ [°]	90	90	90	90
volume [Å ³]	1460.90(13)	3621.06(17)	10908.6(4)	4250.8(5)
Z	4	8	16	8
ρ_{calcd} [g cm ⁻³]	1.540	1.452	1.570	1.502
μ [mm ⁻¹]	1.282	1.048	1.015	1.150
$F(000)$	696	1648	5280	1984
crystal size [mm]	$0.28 \times 0.26 \times 0.15$	$0.24 \times 0.14 \times 0.12$	$0.25 \times 0.20 \times 0.20$	$0.28 \times 0.16 \times 0.06$
θ range for data collection [°]	$3.35 < \theta < 27.51$	$2.58 < \theta < 27.48$	$2.69 < \theta < 27.50$	$2.59 < \theta < 25.06$
limiting indices	$-23 \leq h \leq 23$ $-9 \leq k \leq 9$ $-14 \leq l \leq 14$	$0 \leq h \leq 48$ $0 \leq k \leq 10$ $-16 \leq l \leq 15$	$-24 \leq h \leq 24$ $-24 \leq k \leq 24$ $-29 \leq l \leq 39$	$-12 \leq h \leq 13$ $-14 \leq k \leq 15$ $-33 \leq l \leq 35$
reflections collected	10619	15533	34554	19797
independent reflections	3315 ($R_{\text{int}} = 0.0533$)	4144 ($R_{\text{int}} = 0.051$)	19394 ($R_{\text{int}} = 0.0536$)	7189 ($R_{\text{int}} = 0.0934$)
data/restraints/parameters	3315/0/182	4144/0/218	19394/54/1298	7189/2/487
goodness of fit on F^2	1.040	1.048	1.019	1.004
final R indices [$I > 2\sigma(I)$]				
$R1$	0.0367	0.0377	0.0606	0.0723
$wR2$	0.0837	0.0860	0.1463	0.1627
R indices (all data)				
$R1$	0.0538	0.0635	0.0887	0.1304
$wR2$	0.0925	0.0964	0.1617	0.1912
extinction coefficient	0.0018(13)	0.00062(15)		
largest diff peak/hole [$\text{e} \text{ \AA}^{-3}$]	0.383/−0.419	0.332/−0.443	1.390/−0.742	0.787/−0.586

S.C.B. wishes to thank the Ontario Government for postgraduate scholarships (1998–2002) and Prof. Mike McGlinchey (McMaster University) for helpful discussions. F.J. wishes to acknowledge Deutsche Forschungsgemeinschaft (DFG) for a postdoctoral fellowship, and I.M. is grateful to the Natural Science and Engineering Research Council of Canada (NSERC) for an E. W. R. Steacie Fellowship (1997–1999), the University of Toronto for a McLean Fellowship (1997–2003), the Ontario Government for a PREA Award (1999–2004) and the Canadian Government for a Canada Research Chair (2001–) for the duration of the work described.

- [1] a) S. N. Tandura, M. G. Voronkov, N. V. Alekseev, *Top. Curr. Chem.* **1986**, *131*, 99–189; b) C. Chuit, R. J. P. Corriu, C. Reye, J. C. Young, *Chem. Rev.* **1993**, *93*, 1371–1448; c) R. R. Holmes, *Chem. Rev.* **1996**, *96*, 927–950; d) C. Chuit, R. J. P. Corriu, C. Reye in *The Chemistry of Hypervalent Compounds* (Ed.: K. Akiba), Wiley-VCH, New York, **1999**, pp. 81–146; e) M. Kira, L. C. Zhang in *The Chemistry of Hypervalent Compounds* (Ed.: K. Akiba), Wiley-VCH, New York, **1999**, pp. 147–169.

- [2] a) A. R. Bassindale, Y. I. Baukov, P. G. Taylor, V. V. Negrebetsky, *J. Organomet. Chem.* **2002**, 655, 1–6; b) I. El-Sayed, Y. Hatanaka, S. Onozawa, M. Tanaka, *J. Am. Chem. Soc.* **2001**, 123, 3597–3598; c) T. R. van den Ancker, C. L. Raston, B. W. Skelton, A. H. White, *Organometallics* **2000**, 19, 4437–4444; d) I. El-Sayed, Y. Hatanaka, C. Muguruma, S. Shimada, M. Tanaka, N. Koga, M. Mikami, *J. Am. Chem. Soc.* **1999**, 121, 5095–5096; e) K. Tamao, M. Asahara, T. Saeki, A. Toshimitsu, *Chem. Lett.* **1999**, 335–336; f) J. Belzner, N. Detomi, H. Ihmels, M. Noltemeyer, *Angew. Chem.* **1994**, 106, 1949–1950; *Angew. Chem. Int. Ed. Engl.* **1994**, 33, 1854–1855.
- [3] a) H. Stoeckli-Evans, A. G. Osborne, R. H. Whiteley, *Helv. Chim. Acta* **1976**, 59, 2402–2406; b) W. Finckh, B.-Z. Tang, D. A. Foucher, D. B. Zamble, R. Ziembinski, A. Lough, I. Manners, *Organometallics* **1993**, 12, 823–829; c) K. H. Pannell, V. V. Dementiev, H. Li, F. Cervantes-Lee, M. T. Nguyen, A. F. Diaz, *Organometallics* **1994**, 13, 3644–3650; d) J. K. Pudelski, D. A. Foucher, C. H. Honeyman, A. J. Lough, I. Manners, S. Barlow, D. O'Hare, *Organometallics* **1995**, 14, 2470–2479.
- [4] D. A. Foucher, B.-Z. Tang, I. Manners, *J. Am. Chem. Soc.* **1992**, 114, 6246–6248.
- [5] a) R. Rulkens, A. J. Lough, I. Manners, *J. Am. Chem. Soc.* **1994**, 116, 797–798; b) Y. Ni, R. Rulkens, I. Manners, *J. Am. Chem. Soc.* **1996**, 118, 4102–4114.
- [6] a) Y. Ni, R. Rulkens, J. K. Pudelski, I. Manners, *Macromol. Rapid Commun.* **1995**, 16, 637–641; b) N. P. Reddy, H. Yamashita, M. Tanaka, *Chem. Commun.* **1995**, 2263–2264; c) P. Gómez-Elipse, P. M. Macdonald, I. Manners, *Angew. Chem.* **1997**, 109, 780–783; *Angew. Chem. Int. Ed. Engl.* **1997**, 36, 762–764; d) P. Gómez-Elipse, R. Resendes, P. M. Macdonald, I. Manners, *J. Am. Chem. Soc.* **1998**, 120, 8348–8356; e) K. Temple, F. Jäkle, J. B. Sheridan, I. Manners, *J. Am. Chem. Soc.* **2001**, 123, 1355–1364.
- [7] For a recent review on polyferrocenylsilanes and their properties see: K. Kulbaba, I. Manners, *Macromol. Rapid Commun.* **2001**, 22, 711–724.
- [8] a) M. S. Wrighton, R. G. Austin, A. B. Bocarsly, J. M. Bolts, O. Haas, K. D. Legg, L. Nadjo, M. C. Palazzotto, *J. Am. Chem. Soc.* **1978**, 100, 1602–1603; b) M. S. Wrighton, M. C. Palazzotto, A. B. Bocarsly, J. M. Bolts, A. B. Fischer, L. Nadjo, *J. Am. Chem. Soc.* **1978**, 100, 7264–7271; c) A. B. Fischer, J. B. Kinney, R. H. Staley, M. S. Wrighton, *J. Am. Chem. Soc.* **1979**, 101, 6501–6506.
- [9] J. K. Pudelski, I. Manners, *J. Am. Chem. Soc.* **1995**, 117, 7265–7266.
- [10] a) R. Rulkens, A. J. Lough, I. Manners, *Angew. Chem.* **1996**, 108, 1929–1931; *Angew. Chem. Int. Ed. Engl.* **1996**, 35, 1805–1807; b) F. Jäkle, R. Rulkens, G. Zech, D. A. Foucher, A. J. Lough, I. Manners, *Chem. Eur. J.* **1998**, 4, 2117–2128; c) H. K. Sharma, F. Cervantes-Lee, J. S. Mahmoud, K. H. Pannell, *Organometallics* **1999**, 18, 399–403.
- [11] a) F. Jäkle, R. Rulkens, G. Zech, J. A. Massey, I. Manners, *J. Am. Chem. Soc.* **2000**, 122, 4231–4232; b) T. Baumgartner, F. Jäkle, R. Rulkens, G. Zech, A. J. Lough, I. Manners, *J. Am. Chem. Soc.* **2002**, 124, 10062–10070.
- [12] F. Jäkle, E. Vejzovic, K. N. Power-Billard, M. J. MacLachlan, A. J. Lough, I. Manners, *Organometallics* **2000**, 19, 2826–2828.
- [13] P. Nguyen, G. Stojcevic, K. Kulbaba, M. J. MacLachlan, X.-H. Liu, A. J. Lough, I. Manners, *Macromolecules* **1998**, 31, 5977–5983.
- [14] D. A. Foucher, R. Ziembinski, R. Petersen, J. Pudelski, M. Edwards, Y. Ni, J. Massey, C. R. Jaeger, G. J. Vancso, I. Manners, *Macromolecules* **1994**, 27, 3992–3999. Note that the ^{29}Si NMR shift reported in this paper for [fcSiMePh] (**1b**) is incorrect and should be $\delta = -7.7$ ppm (C_6D_6) not $\delta = -10.9$ ppm.
- [15] B. J. Helmer, R. West, R. J. P. Corriu, M. Poirier, G. Royo, A. de Saxce, *J. Organomet. Chem.* **1983**, 251, 295–298. Although concurrent pseudorotation exchange mechanisms cannot be completely ruled out (e.g. a Berry mechanism) they are unlikely due to the spirocyclic nature of **5a** and **5b**.
- [16] H. Günther, *NMR Spectroscopy*, Thieme, Stuttgart, Germany, **1992**.
- [17] The freezing point of CD_2Cl_2 is -95°C but freezing point depression and kinetic effects can account for the mobility of the solution below this temperature.
- [18] K. Tamao, M. Asahara, T. Saeki, S. Feng, A. Kawachi, A. Toshimitsu, *Chem. Lett.* **2000**, 660–661.
- [19] H. Bock, Z. Havlas, V. Krenzel, *Angew. Chem.* **1998**, 110, 3305–3307; *Angew. Chem. Int. Ed.* **1998**, 37, 3163–3166.
- [20] a) J. C. Green, *Chem. Soc. Rev.* **1998**, 27, 263–272; b) for a study on the influence of strained silacyclobutyl rings on the strength of hypervalent interactions see: M. Spiniello, J. M. White, *Organometallics* **2000**, 19, 1350–1354.
- [21] D. A. Foucher, A. J. Lough, I. Manners, J. Rasburn, J. G. Vancso, *Acta Crystallogr.* **1995**, C51, 580–582.
- [22] K. Tamao, T. Hayashi, Y. Ito, M. Shiro, *Organometallics* **1992**, 11, 2099–2114. Please note that the equation as originally published contains an error and should read: $\% \text{TBP}_e = [1 - (120^\circ - \text{av. eq. angle}) / (120^\circ - 109.5^\circ)] \times 100\%$.
- [23] a) R. Rulkens, D. P. Gates, D. Balaishis, J. Pudelski, D. F. McIntosh, A. J. Lough, I. Manners, *J. Am. Chem. Soc.* **1997**, 119, 10976–10986; b) S. Barlow, M. J. Drewitt, T. Dijkstra, J. C. Green, D. O'Hare, C. Whittingham, H. H. Wynn, D. P. Gates, I. Manners, J. M. Nelson, J. K. Pudelski, *Organometallics* **1998**, 17, 2113–2120.
- [24] K. N. Power-Billard, T. J. Peckham, A. Butt, F. Jäkle, I. Manners, *J. Inorg. Organomet. Polym.* **2000**, 10, 159–168.
- [25] After 12 h **9** is the major product. However, new, broad resonances become visible on the baseline, consistent with ring-opening reactions of **9**. Studies of this chemistry will be discussed in detail in a future publication.
- [26] For previous work on these cationic heterocycles and analogous acyclic species see the following and references contained therein: a) E. Lukevics, I. Segal, A. Zablotskaya, S. Germane, *Molecules* **1997**, 2, 180–185; b) E. Lukevics, S. Germane, I. Segal, A. Zablotskaya, *Chem. Heterocyc. Comp.* **1997**, 33, 234–238; c) Y. Sato, Y. Yagi, M. Koto, *J. Org. Chem.* **1980**, 45, 613–617; d) Y. Sato, H. Sakakibara, *J. Organomet. Chem.* **1979**, 166, 303–307.
- [27] a) F. N. Jones, M. F. Zinn, C. R. Hauser, *J. Org. Chem.* **1963**, 28, 663–665; b) J. T. B. H. Jastrzebski, G. van Koten, *Inorg. Synth.* **1989**, 26, 150–155.
- [28] J. J. Bishop, A. Davidson, M. L. Katcher, D. W. Lichtenberg, R. E. Merrill, J. C. Smart, *J. Organomet. Chem.* **1971**, 27, 241–249.
- [29] D. L. Zechel, K. C. Hultsch, R. Rulkens, D. Balaishis, Y. Ni, J. K. Pudelski, A. J. Lough, I. Manners, *Organometallics* **1996**, 15, 1972–1978.
- [30] Z. Otwinowski, W. Minor, *Methods Enzymol.* **1997**, 276, 307–326.
- [31] G. M. Sheldrick, *SHELXTL/PC V5.1*, Bruker Analytical X-ray Systems, Madison, WI, **1997**.

Received: January 9, 2003 [F4721]